IV. OSCILLATORY AND UNSTEADY PROCESSES IN LIQUID ROCKET ENGINES

by
F.E.C. Culick

The combustion chamber of a propulsion system encloses an astonishing variety of processes. Propellants supplied as gases, liquids or solids undergo physical transformations required as preparation for combustion chiefly in the gas phase. Burning takes place at high pressure in a volume open only to admit the reactants and to exhaust the hot products. As a result of geometry, mixing, and nonuniform properties, the flow field is intrinsically unsteady. The influences of processes unstable at small scales spread to macroscopic levels and become evident as fluctuations of global properties, notably the chamber pressure.

Design considerations for such systems intended for practical applications do not normally include attention to unsteady combustion and flow. Yet unsteady motions are always present, as apparently random fluctuations or noise, and often as coherent oscillatory motions generically called "combustion instabilities." Noisy motions are obvious as vibrations of the structure and as sound emitted both from the structure and from the exhaust flow. Despite the annoyances, and possibly unacceptably high levels of vibration, the amount of energy contained in the random motions is an utterly negligible part of the energy released in combustion of the propellants.

Similarly, excitation and sustenance of a combustion instability normally does not affect the steady performance because the power required to do so is a small part of the total power available from combustion processes. The unsteady motions arise due to an imbalance of energy gains and losses to a small disturbance. If the loss exceeds the gain only by a small amount, the motion is unstable. Hence because combustion processes release high densities of power in a confined volume characterized by relatively small losses of mechanical energy of motion, conditions are favorable for excitation of combustion instabilities and the problem must be anticipated in any new system. Indeed, the chief reason that practical difficulties with combustion instabilities are not worse, is that coupling is relatively weak between combustion processes and unsteady motions: unsteady conversion of heat released in burning to mechanical energy of fluid motion is inefficient.

In practice, the chief undesirable consequences of combustion instabilities are structural vibrations and enhanced heat transfer rates to inert surfaces. Vibrational accelerations may exceed levels tolerable for instrumentation and the payload; in extreme cases, equipment failures may cause termination of flight. Heat transfer coefficients may increase by factors of ten or more, possibly causing structural failure of the combustor. It is often not possible to guarantee that a small amplitude oscillation observed in tests will always remain so in operational engines. Hence, given the very real possibility of failure if large amplitude oscillations occur, as a practical matter there is strong motivation to eliminate combustion instabilities altogether.

To eliminate instabilities requires understanding of the various processes of energy gains and losses and the way in which they combine to produce unstable motions. An observer perceives an unstable motion in a combustion chamber as "self-excited:" The amplitude of the pressure fluctuation grows out of the noise without action of an external influence. Hence the theory of these phenomena belongs to the theory of self-excited dynamic systems. That is essentially the subject of this lecture, cast in the form required for the subject at hand.

Broadly, we may divide the material into three parts: (1) construction of appropriate governing equations; (2) identification and modeling of the dominant physical processes; and (3) application of known mathematical methods to extract results specific to the representation of combustion instabilities. There is no unique strategy. As a part of our discussion here, we describe here an approximate analysis applicable quite generally to combustion instabilities in all types of propulsion systems, and stationary power plants as well. The intent is to produce formulas easy to use and having clear interpretation. Numerical analysis is used to evaluate the formulas to obtain quantitative results; to solve ordinary differential equations; or, in the form of computational

fluid mechanics, to solve the partial differential equations of conservation as a means of assessing the accuracy of the of the approximate results.

We began with a discussion of some general characteristics of combustion instabilities to motivate the form of the analysis developed in the following sections and to provide an elementary context for the more complicated problems of stability treated later.

4.1 REMARKS ON THE STABILITY OF DYNAMIC SYSTEMS

Combustion instabilities are discovered in records of structural accelerations or chamber pressure taken during a test. Figure 4.1 shows a typical pressure record obtained in a laboratory device at CIT. The trace has been filtered to remove the DC component. Figure 4.2 is the power spectral density of that record, exhibiting peaks associated with the presence of several coherent motions. It happens that in this case two acoustic modes of the system were excited and in addition, owing to nonlinear processes, several subharmonics were generated. The organized motions are imbedded in a background of broad band noise. Although the initial growth of the oscillations is not shown in Figure 4.1, other data have shown the approximately exponential increase of amplitude expected for a linearly unstable system.

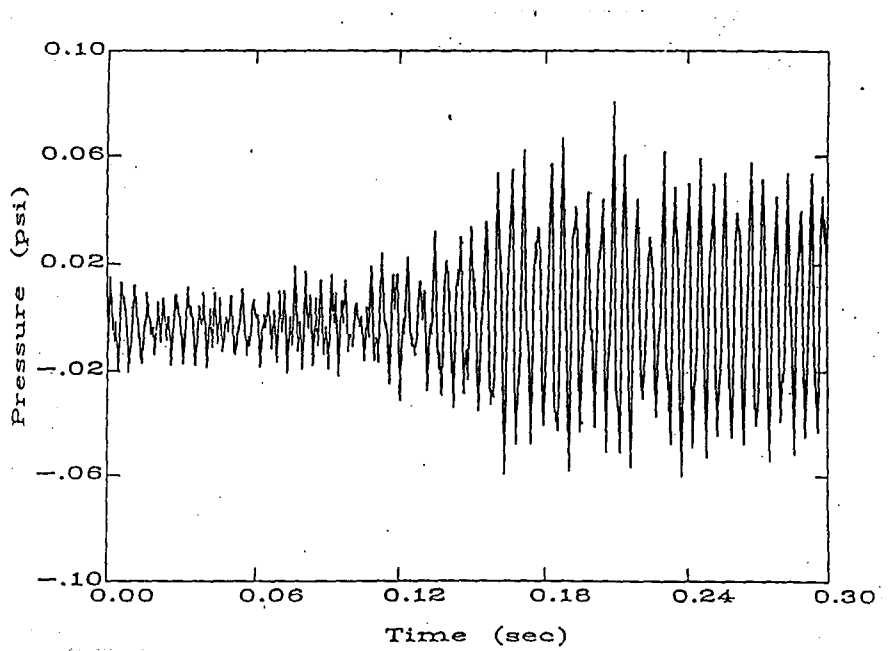

Figure 4.1

A time history like that in Figure 4.1 at first reveals nothing of the system providing the data. It could as well be an electrical system or a purely mechanical device made of spring, masses, dashpots and perhaps a source of energy. The initial growth period will show whether the system is self-excited or driven. The motion in a self-excited system initially grows exponentially in time, varying as $e^{|\alpha|t}$, and reaches a limit cycle only because nonlinear processes are present. An externally driven stable linear system will initially execute a motion whose amplitude varies as $1 - e^{-|\alpha|t}$ and , if the sinusoidal driving force has constant amplitude, will eventually reach a steady oscillatory motion of constant amplitude.

In each of the two cases of linear and nonlinear just described, the average power into the system (energy gains) must equal the average power lost to the system (energy losses) in the long-time steady oscillation.

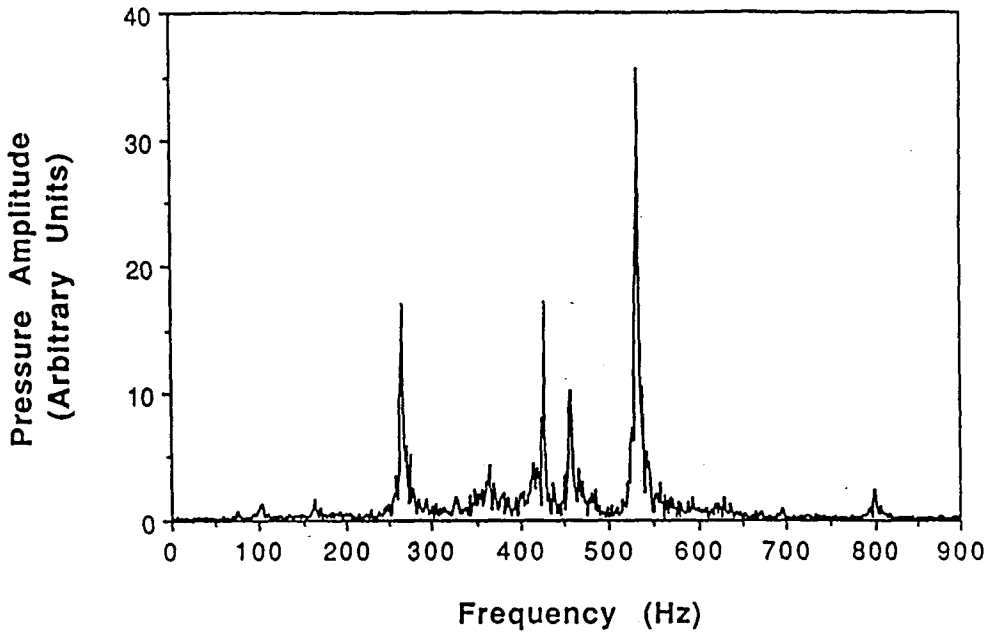

Figure 4.2

As remarked above, the time histories of the two motions after initial transients are negligible, will not show qualitatively any differences that will obviously identify linear or nonlinear behavior. Only detailed analysis of the data will give that information. Moreover, if the motion is dominated by a single frequency, the time record is hardly distinguishable from that one might find for a simple mass/spring/dashpot system.

Yet real pressure records taken for the most complicated real combustion chambers often look like Figure 4.1, an observation based on experience with all types of propulsion systems and stationary power plants as well. Hence it is reasonable to try to construct a representation of combustion instabilities that look much like that for a relatively simple mechanical system. That approach will be described later. By suitable spatial averaging, a nonlinear motion comprising many acoustic modes of a chamber may be represented as a collection of coupled nonlinear oscillators. The representation not only has an appealing form, it is convenient to apply and produces accurate results.

The point here is that there is sound basis for discussing aspects of the behavior found for combustion instabilities, in terms of the behavior of simple oscillators. Thus we suppose first that the motion is dominated by a single oscillator and the pressure fluctuation p' observed at a point in the chamber is assumed to satisfy the equation for a simple forced oscillator:

$$\frac{d^2p'}{dt^2} + 2\alpha_0\frac{dp'}{dt} + \omega_0^2 p' = f\left(p', \frac{dp'}{dt}; t\right) \tag{4.1}$$

The force f may depend linearly or nonlinearly on the pressure, its rate of change and on time. We adopt the convention here that if the system is stable, the constant α is negative and is normally called the decay or attenuation constant. When α is positive it is called the growth constant and a small initial disturbance grows exponentially in time.

It is often true that combustion and flow processes do not cause large changes in frequencies of the modes for a chamber. That is because the frequencies depend mainly on the geometry and on the speed of sound, or the temperature, which is nearly uniform if combustion is well-distributed in the chamber. Hence it is

convenient to assume that α_0 and ω_0 are characteristic of the unperturbed acoustic mode with no combustion or flow (α_0 is therefore negative). Consequently, the force f is associated with interactions between the acoustic mode and the combustion and flow processes. We shall assume throughout that there is no external excitation so we write f in the form:

$$f = 2\alpha_c \frac{dp'}{dt} + \delta\omega^2 p' \tag{4.2}$$

where α_c is the growth constant due mainly to combustion and $\delta\omega^2$ is the frequency shift due to the various processes. Normally $\delta\omega^2 = 2\omega\delta\omega \approx 2\omega_0\delta\omega$ is positive as defined here. Equations (4.1) and (4.2) combine to give

$$\frac{d^2p'}{dt^2} + 2(\alpha_0 - \alpha_c)\frac{dp'}{dt} + (\omega_0^2 - \delta\omega^2)p' = 0 \tag{4.3}$$

The solution for an initial disturbance p'_0 is

$$p'(t) = p'_0 e^{(\alpha_c - \alpha_0)t} e^{i(\omega_0 - \delta\omega)t} \tag{4.4}$$

where we have assumed the usual case, of small frequency shift so

$$\sqrt{\omega_o^2 - \delta\omega^2} \approx \omega_0 \left(1 - \frac{1}{2} \cdot \frac{2\omega\delta\omega}{\omega_0^2}\right) \approx \omega_0 - \delta\omega \tag{4.4}$$

It is also normally true that

$$\frac{|\alpha_c - \alpha_0|}{\omega} \ll 1 \tag{4.5}$$

The general problem of linear stability comes down to finding $\alpha_0, \omega_0, \alpha_c$ and $\delta\omega$. Complications arise in practice because details of the dominant processes are not well known or because modeling of the processes is imprecise. Otherwise the problem of linear stability may be regarded as essentially solved in principle, which is not to say that accurate results can always be obtained in practical applications.

Nonlinear behavior is quite a different matter. There are two fundamental problems to be solved:

(i) The conditions for existence and stability of limit cycles;

(ii) the conditions for nonlinear instability of a linearly stable system.

The second problem has often been called "triggering"; the purpose is to determine how a linearly stable system may execute a stable or unstable limit cycle following a sufficiently large initial disturbance. In contemporary formal language of dynamical systems theory, this is a problem of subcritical bifurcations. It is helpful in making connection with the formalism developed in the following two sections to make a change of notation. The pressure fluctuation p' is actually a function of both time and position in the chambers. As a first approximation we assume the separable form for a single mode,

$$p' = \bar{p}\eta(t)\psi(\vec{r}) \tag{4.6}$$

where $\vec{r}$ denotes position within the chamber. We shall call $\eta(t)$ the amplitude and $\psi(F^0)$ the mode shape. The process of spatial averaging will lead to the oscillator equation for η, similar to (4.1)

$$\ddot{\eta} + 2\alpha_0\dot{\eta} + \omega_0^2\eta = F(\eta, \dot{\eta}, t) = F^{\ell}(\eta, \dot{\eta}) + F^{n\ell}(\eta, \dot{\eta}) \tag{4.7}$$

where F is now a spatially averaged 'force' containing the influences of all physical processes not already accounted for in α_0 and ω_0. Superscripts $(\,)^{\ell}$ and $(\,)^{n\ell}$ refer to linear and nonlinear forces.

If all relevant processes are modelled, the forces F^{ℓ} and $F^{n\ell}$ are known functions of η and $\dot{\eta}$; in this lecture we ignore any explicit dependence on time. For the purpose of this introduction, we suppose that has been done and we assume further that F contains only integral powers of η and $\dot{\eta}$:

$$F(\eta, \dot{\eta}) = 2\alpha_c\dot{\eta} + \beta_1\dot{\eta} + \gamma_1\eta + \beta_2\dot{\eta}^2 + \gamma_2\eta^2 + \cdots \tag{4.8}$$

Equation (4.7) becomes

$$\ddot{\eta} + 2\alpha\dot{\eta} + \omega^2\eta = \beta_2\dot{\eta}^2 + \gamma_2\eta^2 + \beta_3\dot{\eta}^3 + \gamma_3\eta^3 + \cdots \tag{4.9}$$

in which the linear terms of $F(\eta, \dot{\eta})$ have been absorbed in $2\alpha\dot{\eta}$ and $\omega^2\eta$ on the left-hand side. This equation has solutions exhibiting very rich behavior depending crucially on the various parameters $\alpha, \omega, \beta_2, \cdots$ etc. It has received and continues to receive much attention in the literature of dynamical systems theory.

To illustrate some of the nonlinear behavior observed in combustion instabilities we now make some restrictive assumptions and follow a nonrigorous path of reasoning. The pressure oscillations in combustion instabilities commonly have slowly varying amplitude and phase, and the amplitude $\eta(t)$ may be assumed to have the form

$$\eta(t) = r(t)\sin(\omega t + \psi(t)) = A(t)\sin\omega t + B(t)\cos\omega t \tag{4.10}$$

where r, ϕ, A and B are slowly varying in the sense that their fractional changes are small in one cycle of oscillation. Then either by time-averaging or by expansion in two time-scales, we may deduce that two first-order equations for $A(t)$ and $B(t)$:

$$\frac{dA}{dt} = \frac{1}{\tau}\int_t^{t+\tau} F(A,B)\cos\omega t'\,dt'$$

$$\frac{dB}{dt} = \frac{-1}{\tau}\int_t^{t+\tau} F(A,B)\sin\omega t'\,dt' \tag{4.11}a,b$$

When the integrals are carried out, $A(t)$ and $B(t)$ are assumed constant in F. Hence if the form (4.8) is assumed, the right hand sides of (4.11)a,b are power series in A and B. The values of the coefficients — in particular which terms are non-zero — depend critically on the type of nonlinear processes considered. For example, the most thoroughly studied process is nonlinear gasdynamics. In that case, nonlinear terms do not arise if a single mode is assumed; the essence of the problem lies in nonlinear coupling between modes. The equations have a very special structure allowing quite thorough study of the behavior.

Since the purpose here is primarily illustrative, we consider for simplicity, several model problems. They are not necessarily direct counterparts of actual processes but they do capture some important features of possible behavior. With the linear terms shown explicitly, Eqs. (4.11)a,b have the form

$$\frac{dA}{dt} = \alpha A + \theta B + f$$

$$\frac{dB}{dt} = \alpha B - \theta A + g \tag{4.12}a,b$$

where f and g are nonlinear functions of A and B multiply the first by A, and the second by B, and add the result to find

$$\frac{da}{dt} = 2\alpha a + 2(Af + Bg) \tag{4.13}$$

The square of the peak amplitude is $a = A^2 + B^2$ If the nonlinear terms f and g are ignored, the solution to (4.13) is

$$a = a_0 e^{2\alpha t} \quad \text{or} \quad r = r_0 e^{\alpha t} \tag{4.14}$$

where $(\,)_0$ represents the initial disturbance and $r = \sqrt{a}$. When $f = g = 0$, the solutions to (4.12)a,b are

$$A = A_0 e^{\alpha t}\cos\theta t;\; B = B_0 e^{\alpha t}\sin\theta t \tag{4.15}$$

and the amplitude $\eta(t)$, Eq. (4.10), becomes

$$\eta = A_0 e^{\alpha t}\sin(\omega t + \theta) \tag{4.16}$$

Hence the peak values of η vary as $e^{\alpha t}$ and (4.15) gives $r = (A^2 + B^2)^{1/2} \sim e^{\alpha t}$ as already found in (4.14).

Thus the result of time-averaging gives exactly the main results for linear stability. More interesting is nonlinear behavior. To illustrate what one can do is this formulation, we assume first that the right-hand side of (4.13) is quadratic in a:

$$\frac{da}{dt} = 2\alpha a + ba^2 = ka(a_1 - a) \tag{4.17}$$

where $ka_1 = 2\alpha \text{and} k = -b$. The clearest way to see the character of the behavior represented by this equation is to display solution curves in the $(\dot{a}, a)$ plane. Two solutions for $\alpha = ka_1 > 0$ and $\alpha < 0$ are shown in Figure 4.3; we assume a_1 positive.

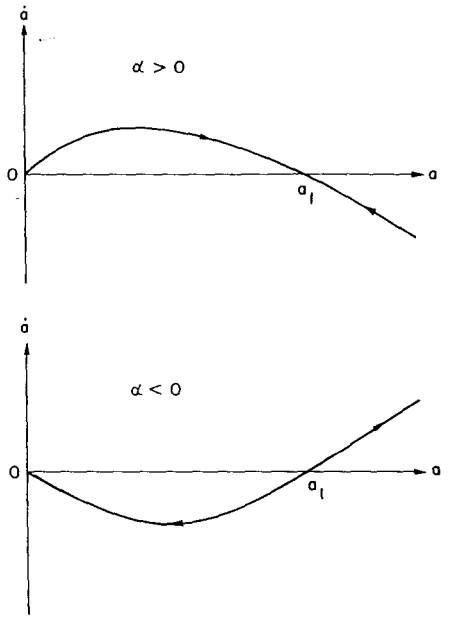

Figure 4.3

The arrows on the curves in Figure 4.3 show the motion of the "state point" representing the time solution of the system following its preparation in some initial state. For $\alpha > 0$ the system is linearly unstable and for any initial state the system eventually executes a limit cycle with amplitude a_1. The point $(a = a_1, \dot{a} = 0)$ represents a stable limit cycle when $\alpha > 0$. On the other hand, that point represents an unstable limit cycle when α is negative. If the initial value a_0 is larger than a_1, the solution grows without limit, and if $a_0 < a_1$, the motion decays to the state of rest, $a = \dot{a} = 0$.

The integral of (4.17) is

$$a = \frac{a_1}{1 + \left(\frac{a_1}{a_0} - 1\right) e^{-\alpha t}} \tag{4.18}$$

If the system is linearly stable ($\alpha < 0$) and $a_0 > a_1$, the amplitude becomes indefinitely large for $t \to \alpha^{-1} \ell n(1 - a_1/a_0)$: the system can be pulsed to an unstable state. This sort of behavior may have been found in early studies of nonlinear behavior in rocket engines.

Pulsing to a stable limit cycle arises if a third-order term is included and instead of (4.17) we have

$$\frac{da}{dt} = ka(a_1 - a)(a_2 - a) \tag{4.19}$$

Typical trajectories for the two cases $k > 0$ and $k < 0$ are shown in Figure 4.4 for which we assume $a_2 > a_1 > 0$. Now the point $(a = a_2, \dot{a} = 0)$ represents a stable limit cycle which can be entered only if the initial amplitude is greater than a_1.

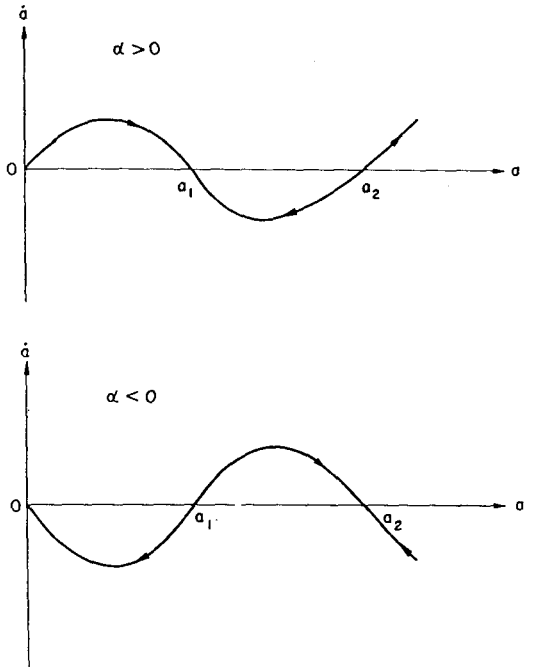

Figure 4.4

The presence of third-order terms is not a guarantee that triggering to a stable limit cycle exists. For example, consider the case when the second order term is missing:

$$\frac{da}{dt} = ka(a_1^2 - a^2) \tag{4.20}$$

The root $a = -a_1 < 0$ is physically inaccessible and the allowed trajectories look like those in Figure 4.3; pulsing to a stable limit cycle does not exist.

All of the above examples arise from systems having a single degree of freedom or, put another way, one mode of motion. Nonlinear terms then represent either "self-coupling" within the modal motion, or the nonlinear response of a source, for example chemical reactions within the volume. If there are two or more degrees of freedom, "cross" or "mutual" coupling may arise, as with nonlinear gasdynamics, and the behavior becomes much more complicated. Not only is the analysis more difficult, but also the results are not easily displayed graphically. The phase space for two modes has four dimensions which, because of an arbitrary phase in the motion, can be reduced to three. To simplify the discussion we now consider two examples for two degrees of freedom, treating the amplitude only.

The first example is nonlinear to second order, and has cross-coupling but no self-coupling term:

$$\frac{da_1}{dt} = \alpha_1 a_1 + b_1 a_1 a_2$$

$$\frac{da_2}{dt} = \alpha_2 a_2 + b_2 a_1^2 \tag{4.21}a,b$$

Note that this is indeed only a model problem for the behavior of two oscillators. We treat only two equations, without showing their rigorous derivation. This amounts partly to ignoring the frequency shifts represented by the linear parameters. We look for a limit cycle in which a_1 and a_2 are constant. In general, oscillatory solutions may also exist, but we ignore that possibility here. The solutions are

$$a_{10} = \pm \left(\frac{\alpha_1 \alpha_2}{b_1 b_2} \right)^{1/2} \qquad a_{20} = -\frac{\alpha_1}{b_1} \tag{4.23}$$

where the subscript $(\,)_0$ now stands for quantities in the limit cycle. Note that for this system a_1 and a_2 must be real, and may be negative. The condition for existence of real solution is

$$\frac{\alpha_1 \alpha_2}{b_1 b_2} > 0 \tag{4.24}$$

For triggering, according to our definition, the system must be linearly stable: α_1 and α_2 must both be negative. Hence the condition for triggering follows from (4.24)

$$b_1 b_2 > 0 \tag{4.25}$$

Now we must determine whether we can find triggering to a stable limit cycle, or whether the solution represents an unstable limit cycle in the sense of Figure 4.3 for $\alpha < 0$. Stability is investigated by considering the time-dependent behavior of small perturbations of the motion a_{10}, a_{20}. Write $a_1 = a_{10} + a_1', a_2 = a_{20} + a_2'$, and substitute into Eqs. $(4.21)a, b$ to find the linearized forms

$$\frac{da_1}{dt} = (\alpha_1 + b_1 a_{20}) a_1' + (b_1 a_{10}) a_2'$$
$$\frac{da_2'}{dt} = (2 b_2 a_{10}) a_1' + (\alpha_2) a_2'$$

Assume solutions varying exponentially in time,

$$a_1' = a_1 e^{\lambda t} \qquad a_2' = a_2 e^{\lambda t}$$

to yield the pair of homogeneous equations

$$(\alpha_1 + b_1 a_{20} - \lambda) a_1 + (b_1 a_{10}) a_2 = 0,$$

$$(2 b_2 a_{10}) a_1 + (\alpha_2 - \lambda) a_2 = 0$$

Nontrivial solutions exist only if the determinant of coefficients vanishes, a condition which gives the characteristic polynomial

$$P(\lambda) = \lambda^2 - \alpha_2 \lambda - 2 \alpha_1 \alpha_2 = 0 \tag{4.26}$$

The product of the roots of this equation is $-2\alpha_1\alpha_2$, which must be negative because $\alpha_1\alpha_2 > 0$. Hence one of the roots has a positive real part. That solution then grows without limit and the limit cycle is unstable. Suppose now that we add self-coupling to the first mode, so Eqs. $(4.21)a, b$ become

$$\frac{da_1}{dt} = \alpha_1 a_1 + b_1 a_1 a_2 + c_1 a_1^2$$
$$\frac{da_2}{dt} = \alpha_2 a_2 + b_2 a_1^2 \tag{4.25}a, b$$

Again assuming a_1, a_2 constant in the limit cycle, we must find a_1 as the solution to the cubic equation

$$a_{10} \left[a_{10}^2 - \frac{c_1 \alpha_2}{b_1 b_2} a_{10} - \frac{\alpha_1 \alpha_2}{b_1 b_2} \right] = 0$$

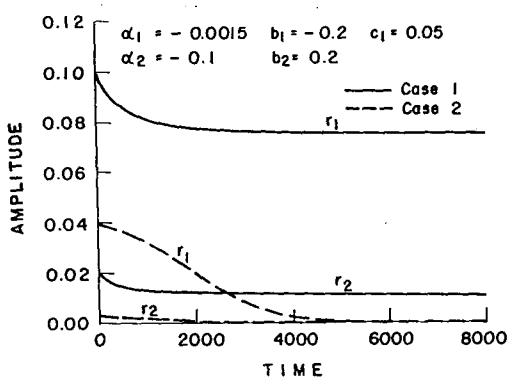

Figure 4.5

The solution $a_{10} = 0$ is of no interest, so

$$a_{10} = \frac{c_1\alpha_2}{2b_1b_2} \pm \left[\left(\frac{c_1\alpha_2}{2b_1b_2}\right) + \frac{\alpha_1\alpha_2}{b_1b_2}\right]^{1/2} \tag{4.26}$$

The solution for a_{20} is

$$a_{20} = -\frac{b_2}{\alpha_2}a_{10}^2 \tag{4.27}$$

In order for a_{10} to be real, the argument in the square root must be positive, giving the condition for existence of limit cycles. Conditions for the stability of this solution lead to the characteristic equation

$$\lambda^2 - (\alpha_1 + b_1a_{20} + 2c_1a_{10} + \alpha_2)\lambda + \alpha_2(\alpha_1 + b_1a_{20} + 2c_1a_{10}) - 2b_1b_2a_{20}^2 = 0$$

This result suggests that with the appropriate choice of the sign and magnitude of c_1, we may be able to cause both roots of this equation to have negative real parts, thereby causing the limit cycle to be stable. Indeed, numerical solutions have established the existence of triggering to a stable limit cycle. Figure 4.5 presents a typical example. If the initial disturbance is less than some threshold value, it decays to zero; otherwise, the disturbance grows to a limit cycle. When $\alpha_1, \alpha_2 < 0$, application of the Routh-Hurwitz criteria establishes necessary and sufficient conditions required for the existence of a stable limit cycle. Hence we conclude that if both cross — and self-coupling are present, a second-order nonlinear system may exhibit triggering to a stable limit cycle.

The preceding examples are intended only to convey the gist of the matter for simple cases. It has certainly not been established that the variable a in these simple models corresponds in any rigorous fashion to the amplitudes a_1, b_1, or $r = (a^2 + b^2)^{1/2}$ arising in more completely formulated problems.

Constructing model equations has been a popular activity in the field of nonlinear dynamical systems, an extremely useful means to suggest the sorts of behavior that might occur. However, there remains always the problem of determining how faithful the model equations actually represent real systems. The purpose of the following two sections is to show how an approximate analysis may be constructed to yield systems of ordinary differential equations realistically applicable to nonlinear combustion instabilities.

4.2 CONSERVATION EQUATIONS FOR TWO-PHASE FLOW

Although the instabilities observed in combustion chambers involve primarily oscillations of the gas phase, it is essential to account for the presence of the liquid phase as well. To simplify the discussion, we lump the

liquid fuel and oxidizer together as a single liquid phase and represent the multi-component gas mixture as a single average gas. Thus we treat a reacting two-phase mixture for which the equations of conservation are:

Conservation of Mass

$$\frac{\partial}{\partial t}(\rho_g + \rho_\ell) + \nabla \cdot (\rho_g \vec{u}_g + \rho_\ell \vec{u}_\ell) = w_{eg} + w_{e\ell} \tag{4.28}$$

Conservation of Momentum

$$\frac{\partial}{\partial t}(\rho_g \vec{u}_g + \rho_\ell \vec{u}_\ell) + \nabla \cdot (\rho_g \vec{u}_g \vec{u}_g + \rho_p \vec{u}_\ell \vec{u}_\ell) = \nabla \cdot \overleftrightarrow{\tau}_g + \vec{m}_{eg} + \vec{m}_{e\ell} \tag{4.29}$$

Conservation of Energy

$$\frac{\partial}{\partial t}(\rho_g e_{g_o} + \rho_\ell e_{\ell_o}) + \nabla \cdot (\rho_g \vec{u}_g \vec{u}_\ell e_{\ell_o}) = \nabla \cdot (\overleftrightarrow{\tau}_g \cdot \vec{u}_g) - \nabla \cdot \vec{q}_g (Q + Q_e) \tag{4.30}$$

Subscript $(\ )_g$ refers to the gas species and subscript $(\ )_\ell$ to the liquid; subscript $(\ )_o$ denotes the stagnation state. External sources are denoted by subscript $(\ )_e$. Those terms do not normally appear in the literature but are included here because they may be used to represent the presence of active control, a subject to be addressed briefly later. The stress tensor $\overleftrightarrow{\tau}_g$ is assumed to depend on properties of the gas phase and may be written as the sum of the isotropic pressure and the viscous stress tensor $\overleftrightarrow{\sigma}_v$:

$$\overleftrightarrow{\tau}_g = -p\overleftrightarrow{I} + \overleftrightarrow{\sigma}_v \tag{4.31}$$

All forces exerted in the flow by external influences are represented by the momentum sources m_{eg} and $m_{e\ell}$. Distributed forces (gravity, electromagnetic, ...) are not an issue in the problems considered here; non-zero values of m_{eg} and $m_{e\ell}$ will arise due to momentum transfer associated with flow of material through the boundary of the combustion chamber and interactions associated with material injected for actuating control. Internal heat flow is represented by $\vec{q}_g$, sufficiently well approximated by Fick's law for the gas phase, and Q represents heat addition in the gas phase associated with combustion processes not accompanying conversion of condensed phase to gas. Hence the symbol e_{g_o} stands for stagnation thermal energy only, containing no part related to chemical processes. For a mixture of perfect gases, each species having constant specific heat,

$$e_{g_o} = C_v T_g + \frac{1}{2} u_g^2 \tag{4.32}$$

where C_v and $\vec{u}_g$ strictly stand for values mass-averaged over all gaseous species.

Let w_ℓ denote the rate at which the liquid phase is converted to gas and Eq. (4.28) can be written as the sum of the two equations:

Conservation of Mass (Gas Phase)

$$\frac{\partial \rho_g}{\partial t} + \nabla \cdot (\rho_g \vec{u}_g) = w_\ell + w_{e_g} \tag{4.33}$$

Conservation of Mass (Liquid Phase)

$$\frac{\partial \rho_\ell}{\partial t} + \nabla \cdot (\rho_\ell \vec{u}_\ell) = -w_\ell + w_{e\ell} \tag{4.34}$$

The following manipulations are directed to writing eventually a nonlinear wave equation governing the behavior of waves in the mixture. Elasticity (the 'spring constant') for wave propagation is provided by the

compressibility of the gas only, while the mass of an elementary oscillator in the medium is the sum of the masses of gas and liquid in a unit volume.

Equation (4.28), the equation for the total density of the mixture, can be rewritten

$$\frac{\partial \rho}{\partial t} + \nabla \cdot (\rho \vec{u}) = \mathcal{W} \tag{4.35}$$

where $\mathcal{W} = -\nabla \cdot (\rho_e \delta \vec{u}_\ell) + w_e$, the total external source of mass, is

$$w_e = w_{eg} + w_{e\ell} \tag{4.36}$$

and the slip velocity between the condensed phase and the gas is

$$\delta \vec{u}_\ell = \vec{u}_\ell - \vec{u}_g \tag{4.37}$$

Now expand the momentum equation, Eq. (4.2), and substitute the definitions to give

Conservation of Momentum (Gas Phase)

$$\rho_g \frac{\partial \vec{u}_g}{\partial t} + \rho_g \vec{u}_g \cdot \nabla \vec{u}_g + \nabla p = \nabla \cdot \overleftrightarrow{\sigma_r} + \vec{F}_\ell - (\vec{\sigma} + \vec{\sigma}_e) + \vec{m}_e \tag{4.38}$$

where

$$\vec{F}_\ell = -\rho_\ell \left[\frac{\partial \vec{u}_\ell}{\partial t} + \vec{u}_\ell \cdot \nabla \vec{u}_\ell \right] \tag{4.39}$$

$$\vec{\sigma} = (\vec{u}_g - \vec{u}_\ell) w_\ell = -\delta \vec{u}_\ell w_\ell \tag{4.40}$$

$$\vec{\sigma}_e = \vec{u}_g w_{e\ell} + \vec{u}_\ell w_{e\ell} \tag{4.41}$$

$$\vec{m}_c = \vec{m}_{eg} + \vec{m}_{e\ell} \tag{4.42}$$

Equation (4.39) is the momentum equation for the condensed phase and σ represents the rate at which momentum is supplied *to* newly created gas phase *by* the gases already present. Hence $-\vec{\sigma}$ in (4.38) represents the force exerted on the gas phase by the vaporizing or evaporating condensed phase. To Eq. (4.38) add $\rho_\ell [\partial \vec{u}_g / \partial t + \vec{u}_g \cdot \nabla \vec{u}_g]$ to find

$$\rho \left[\frac{\partial \vec{u}_g}{\partial t} + \vec{u} \cdot \nabla \vec{u}_g \right] + \nabla p = \nabla \cdot \overleftrightarrow{\tau_v} + \delta \vec{F}_\ell - (\vec{\sigma} + \vec{\sigma}_e - \vec{m}_e) \tag{4.43}$$

where

$$\delta \vec{F}_\ell = -\rho_\ell \left[\frac{\partial \delta \vec{u}_\ell}{\partial t} + \delta \vec{u}_\ell \cdot \nabla \delta \vec{u}_\ell + \delta \vec{u}_\ell \cdot \nabla \vec{u}_g + \vec{u}_g \cdot \nabla \delta \vec{u}_\ell \right] \tag{4.44}$$

is the force of interaction between the condensed and gas phases.

More elaborate manipulations eventually lead to the form of the energy equation for the temperature of the gas phase:

$$\rho \tilde{C}_v \left[\frac{\partial T_g}{\partial t} + \vec{u}_g \cdot \nabla T_g \right] + p \nabla \cdot \vec{u}_g = (\overleftrightarrow{\sigma_v} \cdot \nabla) \vec{u}_g - \nabla \cdot \vec{q}_g + (Q + Q_e) + \vec{u}_g \cdot (\vec{\sigma} + \vec{\sigma}_e - \vec{m}_e)$$
$$+ \delta Q_\ell + w_\ell \delta e_o + \delta \vec{u}_\ell \cdot \vec{F}_\ell (e_{g_o} w_{eg} + e_{\ell o} w_{e\ell}) \tag{4.45}$$

where

$$Q_\ell = -\rho_\ell \left[\frac{\partial e_\ell}{\partial t} + \vec{u}_\ell \cdot \nabla e_\ell \right]$$
$$\delta e_o = e_{\ell_o} - e_{g_o} \tag{4.46}$$

and, corresponding to (4.44), the heat exchange between the two phases is

$$\delta Q_\ell = -\rho_\ell C \left[\frac{\partial \delta T_\ell}{\partial t} + \delta \vec{u}_\ell \cdot \nabla \delta T_\ell + \delta \vec{u}_\ell \cdot \nabla T_g + \vec{u}_g \cdot \nabla \delta T_\ell \right] \tag{4.47}$$

The mass-averaged properties are

$$\bar{C}_v = \frac{1}{\rho}(\rho_g C_v + \rho_\ell C) = \frac{C_v + C_m C}{1 + C_m}$$
$$\bar{C}_\ell = \frac{1}{\rho}(\rho_g C_\ell + \rho_\ell C) = \frac{C_v + C_m C}{1 + C_m} \tag{4.48}a,b$$

and $C_m = \rho_\ell / \rho$ is the liquid phase loading, the fraction of mass in unit volume as liquid.

In summary, the three basic equations for unsteady motions in a two-phase mixture are:

Conservation of Mass
$$\frac{D\rho}{Dt} = -\rho \nabla \cdot \vec{u} + \mathcal{W} + \mathcal{W}_e \tag{4.49}$$

Conservation of Momentum
$$\rho \frac{D\vec{u}}{Dt} = -\nabla p + \vec{\mathcal{F}} + \mathcal{F}_e \tag{4.50}$$

Conservation of Energy
$$\rho C_v \frac{DT}{Dt} = -\rho \nabla \cdot \vec{u} + \mathcal{Q} + \mathcal{Q}_e \tag{4.51}$$

where the sources are

$$\mathcal{W} + \mathcal{W}_e = -\nabla \cdot (\rho_\ell \delta \vec{u}_\ell) + w_e \tag{4.52}$$
$$\vec{\mathcal{F}} + \vec{\mathcal{F}}_e = \nabla \cdot \overleftrightarrow{\sigma_v} - \vec{\sigma} + \delta \vec{F}_\ell - (\sigma_e - \vec{m}_e) \tag{4.53}$$
$$\mathcal{Q} + \mathcal{Q}_e = (\overleftrightarrow{\sigma_v} \cdot \nabla)\vec{u} - \nabla \cdot \vec{q}_g + Q + \vec{u} \cdot \vec{\sigma}_e + \delta Q_\ell + \delta e_o w_\ell + \delta \vec{u}_\ell \cdot \vec{F}_\ell + Q_e + \vec{u} \cdot (\vec{\sigma}_e - \vec{m}_e) - (e_{g_o} w_{e_g} + e_{\ell_o} w_{e_\ell}) \tag{4.54}$$

To simplify writing, we shall hereafter use the symbol $\vec{u}$ instead of $\vec{u}_g$ for the gas velocity; T instead of T_g for the gas temperature; and we drop the overbars on mass-averaged thermodynamic properties. The substantial derivative is defined in terms of the gas velocity,

$$\frac{D}{Dt} = \frac{\partial}{\partial t} + \vec{u} \cdot \nabla \tag{4.55}$$

The equation of state appropriate to this formulation is

$$p = \rho R T_g \tag{4.56}$$

where R is the mass-averaged gas constant $\bar{C}_p - \bar{C}_v$, equal to ρ_g / ρ times the gas constant for the gas mixture. From the preceding equations, the equation for the pressure can be derived:

$$\frac{Dp}{Dt} = -\gamma p \nabla \cdot \vec{u} + \mathcal{P} + \mathcal{P}_e \tag{4.57}$$

with

$$\mathcal{P} + \mathcal{P}_e = \frac{R}{C_v} Q - RT \nabla \cdot (\rho_p \delta \vec{u}_\ell) + p \frac{D \ln R}{Dt} + \left(\frac{R}{C_v} Q_e R T w_e \right) \tag{4.58}$$

Equations (4.49) – (4.57) and the equations of state (4.56) describe the motions of the two-phase mixture. Possibly with small modifications or extensions to accommodate many species, these are the basic equations for all analyses of combustion instabilities. To obtain solutions, in addition to setting boundary conditions, the condensed phase must be treated separately with Eqs. (4.34), (4.39), and (4.47), with suitable laws for the force and heat exchange between the two phases.

4.3 THE WAVE EQUATION FOR COMBUSTION INSTABILITIES

A wave equation may be constructed by analogy with a procedure followed in classical acoustics. Because we shall not deal with nonlinear behavior in the analysis described in this paper, we shall work from the beginning with the linearized forms of the governing equations. Write all variables as sums of mean and fluctuating parts, $p = \bar{p} + p'$, etc. and assume that the mean values are independent of time. Substitute in (4.50) and (4.57) and ignore terms of second order and higher in the fluctuations to find

$$\bar{\rho}\frac{\partial \vec{u}'}{\partial t} = -\nabla p' + \vec{\mathcal{F}}' + \vec{\mathcal{F}}'_e$$

$$\frac{\partial p'}{\partial t} = -\gamma\bar{p}\nabla\cdot\vec{u}' - \gamma p'\nabla\cdot\vec{\bar{u}} - \bar{u}\cdot\nabla p' + \mathcal{P}' + \mathcal{P}'_e \qquad (4.59)a,b$$

To simplify things, we have assumed also that the mean pressure and density are uniform. Now differentiate (4.59)b with respect to time, substitute (4.59)a, and re-arrange the result to find

$$\nabla^2 p' - \frac{1}{\bar{a}^2}\frac{\partial^2 p'}{\partial t^2} = h + h_e \qquad (4.60)$$

where

$$h + h_e = -\bar{\rho}\nabla\cdot(\vec{\bar{u}}\cdot\nabla\vec{u}' + \vec{u}'\cdot\nabla\vec{\bar{u}}) + \frac{1}{\bar{a}^2}\vec{\bar{u}}\cdot\nabla\frac{\partial p'}{\partial t}$$
$$+ \frac{\gamma}{\bar{a}^2}\frac{\partial p'}{\partial t}\nabla\cdot\vec{\bar{u}} + \nabla\cdot\vec{\mathcal{F}}' - \frac{1}{\bar{a}^2}\frac{\partial \mathcal{P}'}{\partial t} + \nabla\cdot\vec{\mathcal{F}}'_e - \frac{1}{\bar{a}^2}\frac{\partial \mathcal{P}'_e}{\partial t} \qquad (4.61)$$

Terms identified by subscript $(\ )_e$ always correspond, so h_e is defined as the last two terms on the right hand side.

The boundary condition is set on the normal gradient of the pressure by taking the scalar product of (4.59)a with the outward normal vector, giving

$$\hat{n}\cdot\nabla p' = -f - f_e \qquad (4.62)$$

where

$$f + f_e = \bar{\rho}\frac{\partial \vec{u}'}{\partial t}\cdot\hat{n} + \bar{\rho}(\vec{\bar{u}}\cdot\nabla\vec{u}' + \vec{u}'\cdot\nabla\vec{\bar{u}})\cdot\hat{n} - \vec{\mathcal{F}}'\cdot\hat{n} - \vec{\mathcal{F}}'_e\cdot\hat{n} \qquad (4.63)$$

The first term is commonly rewritten by introducing a response or admittance function characterizing the unsteady behavior of the boundary in response to imposed fluctuations. That it is the normal acceleration that matters (or frequency times velocity for sinusoidal disturbances) suggests correctly that the boundary appears as a fluctuating diaphragm (a 'speaker') to the unsteady field in the volume.

Otherwise, only gasdynamical interactions between the mean and fluctuating velocity fields are shown explicitly in (4.60) – (4.63). All other processes are hidden in $\mathcal{P}'$ and $\vec{\mathcal{F}}'$, those directly associated with external (control) actions being contained in $\vec{\mathcal{F}}'_e$ and $\mathcal{P}'_e$.

4.4 UNSTEADY PROCESSES IN LIQUID ROCKET ENGINES

The formulation of the approximate analysis described in the preceding two sections is applicable quite generally to combustion instabilities in any propulsion system, as well as in stationary powerplants. Fundamentally, differences in unsteady phenomena observed in the various systems arise chiefly for two reasons; geometries differ, and the types of propellants and the way in which they are supplied differ among the systems. Consequently, although generally we are concerned with the excitation and sustenance of unsteady motions in a compressible gas - comprising chiefly the products of combustion - the mechanisms causing the motions will vary widely.

In liquid rocket engines, we may for convenience, divide the processes other than gas dynamics into four classes: The flow in the feed system, injection processes, combustion processes and unsteady flow through the exhaust nozzle. There is a large body of literature associated with each of these topics and our intention here is mainly to call attention to the basic phenomena. It is impossible and inappropriate to provide a detailed coverage.

4.4.1 Flow in the Feed System

Oscillations in the propellant supply may occur for at least three reasons: The flows may themselves contain hydrodynamic instabilities; rotating machinery used to pump the flows may introduce serious fluctuations (e.g., due to flow separation in cavitation) and vibrations of the supporting structure may cause oscillations of the flows.

Coupling between pressure oscillations in the combustion chamber, structural vibrations and oscillations of the fuel supply (which then couple to the combustion processes in the chamber) comprise a well-known phenomenon called the POGO instability.

During the 1960s, the POGO instability received much attention as a serious problem in several vehicles including the Thor, Atlas, and Titan vehicles. Rubin (Ref. 4.1) has given a clear brief summary, including particular emphasis on pump cavitation and wave propagation in the propellant feed lines. Those are matters often overlooked by those concerned with motions in the combustion chamber. Yet they provide significant contributions to time lags in the system.

More recent work in France has been reported by Dordain, Lourme and Estoureig (Ref. 4.2) for the Europa II and Diamant B vehicles.

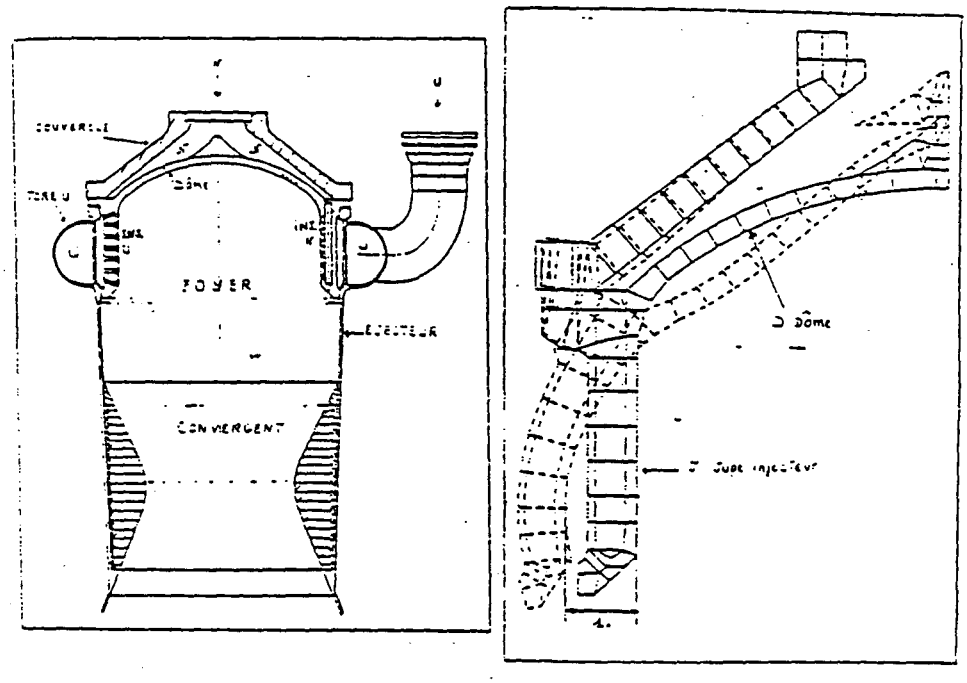

Figure 4.6

A different kind of instability arising from structural vibrations was discovered after the failure of an Ariane vehicle due to the instability in a Viking engine. The problem causing the failure involved coupling between

the pressure oscillations in the chamber and structural vibrations of the injector which is placed in the lateral boundary. Figure 4.6, taken from Souchier, Lemoine and Dorville (Ref. 4.3), shows the computed distortion of the injector plane. As a result, the fuel and oxidizer jets were shaken, causing (apparently) perturbations of the distribution and phase of the energy release, thereby closing the loop and making possible self-excited motions. It is important to understand that in this case, oscillations of the mass flux in the supply lines need not be present to cause instabilities. If the chamber walls distort, motions of the injection elements cause fluctuations in the spatial distribution of injected propellants and hence of the combustion processes. Those events affect directly, the coupling with acoustic waves, leading, possibly , to combustion instabilities.

4.4.2 Injection Processes

The term 'injection processes' is used here to mean those events subsequent to the supply of propellants to the injection elements and prior to vaporization, mixing and combustion in the gas phase. That is, we mean to capture those processes that are particularly sensitive to the design of the injector. Because details of these processes are discussed more thoroughly in Lectures 3 and 6, we limit ourselves here to a brief description of the subject. Several of the papers in Ref. 4.4 are particularly good, recent reviews.

Several smaller classes of processes can be conveniently identified within the broad category of injection processes:

(a) unsteady phenomena within the injector

(b) interactions of liquid streams and of liquid and gas streams

(c) formation of liquid sheets and droplet formation

(d) infractions among droplets, secondary breakup, coalescence and other processes in a nonreacting spray, including the influences of turbulent flow

Which of these processes dominate depends very much on the sort of injector involved. There seem generally to be three kinds mainly of interest for liquid rocket engines; they are distinguished by the configurations of the liquid when they are discharged by the injection elements into the combustion chamber:

(1) impinging jets

(2) concentric jet (coaxial injection)

(3) jet/sheet (non-coaxial)

The last case occurs in pintle injectors, notably that used in the TRW Lunar Descent Module Engine.

Figure 4.7, taken from the Spring 1989 issue of the Rocketdyne publication *Threshold*, shows the common configurations of injector elements. Figure 4.8 is a photograph of the behavior in a spray formed by impinging jets of water at room temperature. Immediately following impingement, a spray fan or sheet is formed. Either because of disturbances already growing in the jets, or because the sheet is itself unstable (possibly for both reasons), the sheet breaks up. There are several forms of the break-up, but in any event a cloud of liquid drops or droplets is formed, having a fairly broad distribution of size and velocities. Because there is a surrounding atmosphere of moving gases, the sheet and the drops are subject to shear forces that encourage break-up of both. In a combustion chamber, these processes take place in an atmosphere consisting of combustion product gases and reactant gases as well. In the F-1 Apollo engine, for example, the liquid oxygen vaporized much more rapidly than the RP-1 hydrocarbon fuel. Under these circumstances, the picture presented by a test involving, say, two jets of water at room temperature, does not reproduce faithfully the situation in the chamber.

Figure 4.8 suggests the general character of the development of a liquid sheet and the formation of droplets, items (b) – (d) listed above, but shows nothing of events within the injector. In fact, the internal geometry of injector elements can create an acoustical system having resonances in the frequency range of

Common Injection Element Configurations

Element Designation	Element Configuration (Flow Direction)	Characteristics	Engine Application
Concentric Tube	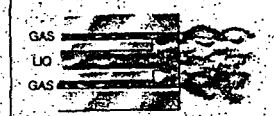	• Very good wall compatibility • Very high performance with LOX/H_2 • Good stability characteristics with LOX/H_2 • Fuel is gas • Small annular gap requires care in fabrication and is sensitive to contamination	• Shuttle main and preburners • J-2 • Orbit Transfer Vehicle
Concentric Tube with Liquid Swirl	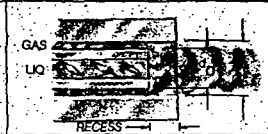	• Same as concentric tube except: • Improved mixing and atomization • More complex element • Stability characteristics in large engines unknown • Possible wall compatibility issue with some designs • Gas can also be swirled	• RL-10
Unlike Pentad (4 on 1)		• Applicable to very high or low mixture or density ratios • Good mixing and atomization • Difficult to manifold	• Experimental
Unlike Doublet (1 on 1)	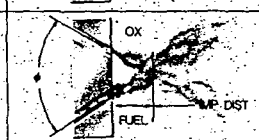	• Good overall mixing and atomization (High Performance) • Simple to manifold • Subject to blowapart with hypergolic propellants	• LEM ascent engine • Delta launch vehicle • Almost all high response attitude control engines using storable propellants
Unlike Triplet (2 on 1)		• Good overall mixing and atomization (High Performance) • Symmetric spray pattern • Subject to blowapart with hypergolic propellants • Fuel can be gas • Pattern can be reversed	• Agena upper stage • Rocketdyne LEM descent engine design • LOX/RPI gas generators
Like Doublet (1 on 1)	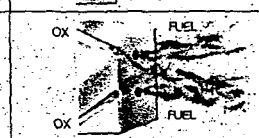	• Easy to manifold • Excellent for chamber wall compatibility • Not subject to blowapart • Less effective atomization and mixing than unlike impinging elements	• Titan I and II first stage • Redstone, Jupiter, Thor, Atlas boosters • Shuttle OMES • H-1, F-1 engines
Showerhead	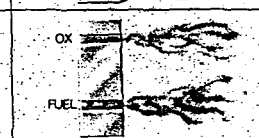	• Often employed for fuel boundary layer cooling of chamber wall • Easy to manifold • Poor atomization and mixing (Low Performance)	• Aerobee sustainer • X-15 • Pioneer
Variable Area (Pintle)	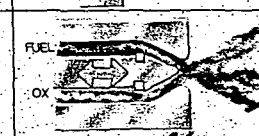	• Throttleable over wide range • Complex fabrication • Lower performance	• LEM descent engine • Lance sustainer
Splash Plate	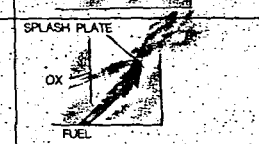	• Less sensitive to design tolerances • Generally larger elements	• Lance booster (early version) • Saturn SIVB ullage control • Apollo CM RCS (SE-6) • Gemini SC maneuvering attitude control and reentry engines

Figure 4.7

oscillations in the chamber. The phenomenon has been known since it was first definitely identified in the J-2S LOX/hydrogen engine used in the Apollo engine, although the problem had been present in earlier work. Reference 4.5 is a recent discussion containing the most detailed analysis of the problem.

It seems accurate to state that the greater part of what is known about the events in which liquid jets are transformed to drops has been learned from tests with liquids at room temperature and with no combustion. While it is true that such tests are necessary, valuable, and do produce a great deal of useful information, one must never forget that the situation may be drastically different when combustion occurs. Heat transfer

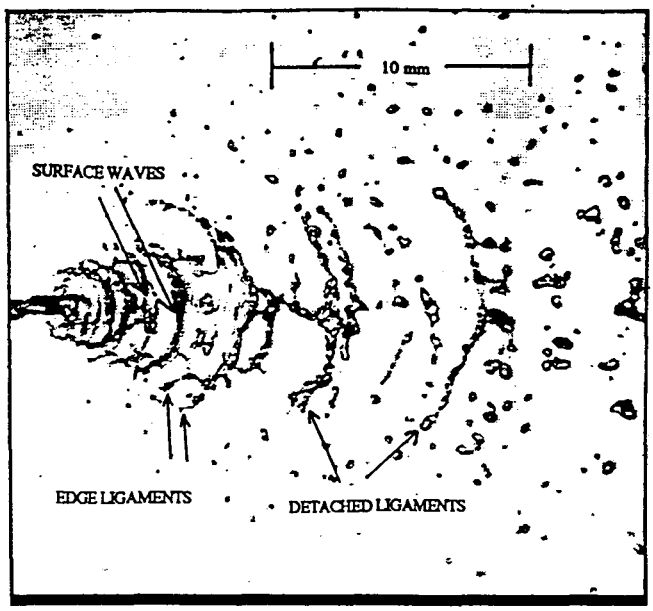

Figure 4.8

upstream and pressure disturbances generated by combustion of individual drops may have strong effects on the jets and spray sheets before and during break-up. For example, with hypergolic propellants, 'blow-a-part' of the reactive streams and 'popping' or intermittent explosion of liquid may be sufficiently vigorous to excite instabilities.

Whatever may be the environment, the first step in the transformation of liquid jets to drops must involve some sort of instability. For the case of impinging jets, the jets themselves may be unstable (a single jet breaks into drops) or the spray fan is unstable. Concentric jets are unstable at their interface. The basic processes responsible for the instabilities are characterized by various dimensionless groups that provide scaling laws. See Refs. 4.6 and 4.7 for particularly good discussions of scaling.

Determining the distributions of drop size and velocity theoretically is an extremely difficult problem, more so than the matter of incipient instability. In general, the influences of aerodynamic forces on the break-up of sprays and secondary break-up of drops is so complicated as to be beyond realistic analysis.

4.4.3 Vaporization, Mixing, and Combustion Processes

Combustion occurs in the gaseous phase and must be preceded by vaporization and mixing. In a LOX/ hydrocarbon system, such as in the F-1, vaporization of the liquid oxygen occurs much more rapidly than that of the liquid fuel. Hence a significant part of the spray combustion involves vaporization and subsequent combustion of the fuel in an oxygen-rich atmosphere. It appears that some of the consequences of detailed design changes on the injector elements may be explained ultimately by the large difference in vaporization rates. That characteristic must also have much to do with differences in the stability of concentric injectors compared with impinging jets when the same propellant combination is used.

The situation for a cryogenic system is less clear, the vaporization rates of LOX and LH2 being closer than those of LOX and a hydrocarbon fuel. Available information is insufficient to allow general characterization.

All the processes discussed to this point have to do mainly with questions of fluid mechanics, or hydraulics, and depend primarily on the physical properties of density, viscosity, surface tension and, to a lesser extent,

thermal conductivity. Most of the significant phenomena can be well understood by considering a single, pure liquid (thereby excluding, of course, combustion) and without wide variations of temperature and pressure. Thus, experiments at room temperature and pressure with various inert liquids provide a great part of the fundamental data required and in fact much work remains before the subjects of jet break-up, jet impingement and formation of sheets, disintegration of sheets, and the formation of drops from sheets can be considered well-understood.

While burning of single drops has been actively studied for many decades and is quite well understood, spray combustion, particularly for dense clouds of interacting drops under conditions found in a rocket chamber, is very poorly understood. Only *ad hoc* modeling is available for unsteady combustion of sprays.

In addition to the purely fluid-mechanical and chemical (i.e. combustion) problems, serious further complications arise in combustion chambers operated at high pressure, namely those arising from behavior near the critical point. This is not a new subject, but thorough analysis for conditions appropriate to combustion instabilities in liquid rocket engines is recent and unfinished.

The fundamental origin of the special behavior accompanying combustion near the critical point is the rapid variation of thermodynamic properties, particularly the mass diffusivity and the latent heat of vaporization. For a given substance or mixture of substances, the pressure p_{cr} and the temperature T_{cr} at the critical point are well-defined. However, the special characteristics of behavior at the critical point itself, extend, albeit attenuated, in some region about the critical point. Hence it is quite clearly unnecessary that the chamber pressure and temperature be precisely p_{cr} and T_{cr} to cause unusual phenomena during combustion. Moreover, at a given pressure, the temperature near a vaporizing or burning liquid drop varies from the ambient value in the immediate environment to some value within the liquid.

To be specific, consider a liquid drop of oxygen injected as liquid, and hence having temperature below the critical point, into a hot fuel-rich environment, the simplest case being hot hydrogen. Suppose that the chamber pressure is the critical value for some mixture of the fuel and oxidizer. As the drop follows its trajectory, its temperature rises, oxygen vaporizes, and gaseous hydrogen diffuses inward. Somewhere between the center of the drop and the environment far away, the temperature and pressure may, if conditions are suitable, assume the critical values for the local mixture ratio of oxygen and hydrogen. For a spherically symmetric flow, the critical point is reached on a spherical surface. Locally, the sharp variations of properties with temperature will produce drastic changes in the flow field at and near that surface. Globally, those effects have substantial influence on the steady burning rate.

If oscillations of pressure and temperature occur in the environment, then it is possible, even though the average chamber pressure may be far from critical, that critical conditions are reached in some point of the drop under unsteady conditions. Then transient fluctuations can be amplified by the large fluctuations of thermodynamic properties. The result is a new possibility for coupling between acoustical motions in the chamber and droplet burning.

The most thorough analysis of steady burning under supercritical conditions has been covered recently in Refs. 4.8, 49, and 4.10. As the preceding remarks suggest, calculations in which supercritical behavior is ignored are seriously in error when the environmental conditions are near the critical point. Less has been accomplished for unsteady behavior.

4.4.4 Unsteady Flow in Exhaust Nozzles; The Nozzle Response Function

When a steady wave is incident upon a choked exhaust nozzle, it is partly transmitted and partly reflected. At first acquaintance, it is a surprising result that the conventional convergent-divergent nozzle appears to the wave system in the chamber to be more like a reflecting rigid wall than like an open hole. The reason is that the incident acoustic wave is subject to strong interactions with mean properties rapidly varying along the axis and as a result strong reflections are created. The overall reflection coefficient is to first order, proportional to the Mach number of the mean flow entering the nozzle.

Tsien (Ref. 4.11) published the first work on the subject elaborate by Crocco and his colleagues (Refs. 4.12, 4.13, and 4.14) for purely axial oscillations. Culick (Ref. 4.15) and Crocco and Sirignano (Ref. 4.16) computed the nozzle response function for transverse waves in a cylindrical chamber. In all cases the nozzle attenuates waves, except under some conditions for transverse waves. The possibility that incident transverse waves might be amplified has never been confirmed experimentally, although the available data suggest that the theory for small-amplitude waves is quite accurate.

The damping supplied by a choked nozzle is normally a significant contribution to the stability of waves in a combustion chamber. In fact, a good approximation for practical purposes is the result obtained for short or 'compact' nozzles (short compared to a wavelength of the wave in the chamber). In that case, the flow in the nozzle may be assumed to respond quasi-statically; the result is that the ratio of the fractional change of mass flux and the pressure fluctuation, defined as the nozzle response function, is

$$\frac{m'/\bar{m}}{p'/\gamma\bar{p}} = \overline{M}_e \tag{4.64}$$

4.4.5 The Time-Lag Representation of Combustion Processes

The basic idea of the time-lag model is simple, and quite general, related to the familiar experience that a forced oscillating system will gain energy if the force has a component in phase with the velocity of the point of application. Stability of dynamical systems characterized in some sense by a phase or time lag had been studied prior to the concern with combustion instabilities. In 1941, Summerfield (Ref 4.17) had observed low frequency 'chugging" during firings of a liquid rocket. Discussion with von Karman led to the idea of a time lag as a possible explanation. Gunder and Friant (Ref 4.18) independently introduced a time lag in their analysis of chugging, but it was Summerfield's paper and subsequent work at Princeton by Crocco that established the time lag theory in the form widely used.

The essential idea in all applications of the time lag is that a finite interval — the lag — exists between the time when an element of propellent enters the chamber and the time when it burns and releases its chemical energy. Such a time lag must exist in steady operation, and, since combustion is distributed throughout the chamber, there is no unique value. Evidently a complete analysis of injection and subsequent processes could then be interpreted in terms of a time lag; results exist only for approximate analyses.

Now suppose that at time t the pressure in the chamber suddenly decreases, causing an increase in the flow of propellant through the injector. The increased mass burns at some later time $t + \tau$, where τ is the time lag. If the pressure is increasing when the added mass burns, the energy released will tend to encourage the pressure increase, a destabilizing tendency. This elementary process is easily interpreted with Rayleigh's criterion. Assume that the pressure varies sinusoidally,

$$p' = \hat{p}\sin\omega t \tag{4.65}$$

and that the energy occurs later with constant time lag τ,

$$Q' = \hat{Q}\sin\omega(t-\tau) \tag{4.66}$$

Integration of the product $p'Q'$ over one period $2\pi/\omega$ gives

$$\int_t^{t+2\pi/\omega} p'Q'dt' = \hat{p}\hat{Q}\int_t^{t+2\pi/\omega} \sin\omega t'\sin(\omega t'-\omega\tau)dt' = \hat{p}\hat{Q}\frac{\pi}{\omega}\cos\omega\tau \tag{4.67}$$

Thus, according to Rayleigh's criterion, Section 4.8.1, we expect that net energy is added to the oscillation if $\cos\omega\tau$ is positive, so the time lag must lie in the ranges

$$0 < \tau < \frac{\pi}{2\omega}, \quad \frac{3\pi}{2\omega} < \tau < \frac{5\pi}{2\omega}, \quad \ldots\text{etc.} \tag{4.68}$$

Suppose that the system is unstable and that τ lies in the range $3\pi/2\omega < \tau < 5\pi/\omega$. Then the strategy for fixing the problem is based on modifying the system so that τ is either increased or decreased, placing its value outside the range for instability.

Because the processes subsequent to injection are surely dependent on the flow variables, pressure, temperature, velocity, ..., it is unrealistic to assume that the time-lag is constant. The most widely used form of the representation with a time lag are dominated by its dependence on pressure.

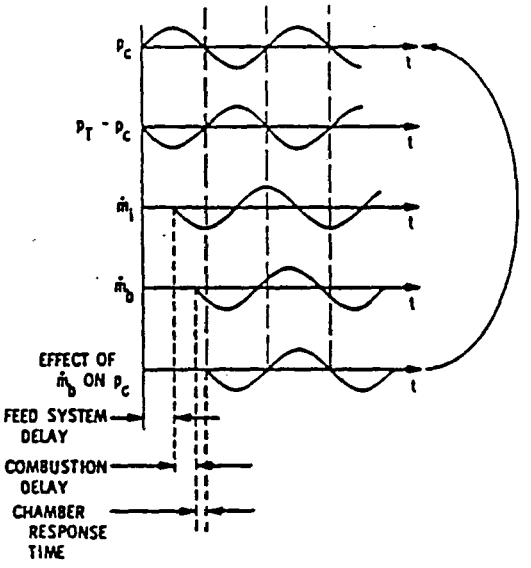

Figure 4.9

Figure 4.9, taken from Ref 4.19, is a sketch illustrating the behavior for a sinusoidal pressure oscillation imposed on the system. The total time delay to burning is supposed in this case to be composed of two parts, due to the propellant feed system, and the combustion delay (injection, atomization, vaporization, mixing, and chemical kinetics). It is the second part that is sensitive to the flow conditions in the chamber.

Let $\dot{m}$ denote the mass flow (mass/sec) of propellant. At this point we are not concerned with details and we need not distinguish between fuel and oxidizer. The arguments based on the idea of a time lag are directed mainly to constructing a representation of the mass source term $w_l(mass/vol-sec)$ in the continuity equation. Thus the result is intended to express the rate of conversion of liquid to gas in a volume element of the chamber. These is no consideration of combustion processes; the usual assumption is that combustion occurs instantaneously, a view that determines how the time lag model ought to be incorporated in the equations.

Let ($\vec{r}$, dV) denote the volume element at position $\vec{r}$ in the chamber and let (t, dt) denote the small time interval dt at time dt. The idea is that the amount of liquid $w_l dV dt$ converted to gas in the element (r, dV) in the interval (t, dt) was injected as $\delta\dot{m}(t-\tau)d(t-\tau)$ at the time $t-\tau$ in the interval $d(t-\tau)$. Hence by conservation of mass,

$$w_l dV dt = \delta\dot{m}_i(t-\tau)d(t-\tau) \tag{4.69}$$

According to earlier remarks, the time lag is supposed to be variable, and can be written as the sum of average and fluctuating values, $\tau = \bar{\tau} + \tau'$. In steady-state operation, (4.69) is

$$\bar{w}_l dV dt = \delta\dot{m}_i(t-\bar{\tau})d(t-\bar{\tau}) = \delta\dot{m}_i(t-\bar{\tau})dt \tag{4.70}$$

Expanding $\delta\dot{m}(t-\tau)$ in Taylor series for use in (4.69) we have

$$\delta\dot{m}_i(t-\tau) = \delta\dot{m}_i(t-\bar{\tau}) + \tau'[\frac{d}{dt}\delta\dot{m}_i(t)]_{t-\tau} + \cdots \tag{4.71}$$

The second term is non-zero if the injected mass flow is not constant. There are many situations (notably for low frequency instabilities) for which variations are important. But for the instabilities at high frequencies, variations of the propellant flow are generally not important. Hence we ignore the second term in (4.71) and substitute (4.70) in (4.69) to find

$$w_l(\vec{r},\ t) = \bar{w}_l\left(1 - \frac{d\tau}{dt}\right) \tag{4.72}$$

The variations of the local conversion of liquid to gas depend in this simple fashion on the time-dependence of the time lag. Note that τ may in general depend on position: the reasoning here is quite widely applicable.

The difficult problem is of course to predict τ — in fact it has never been done. Crocco introduced the idea that the time lag is the period required for the processes leading to vaporization to be completed. He assumed that this integrated effect can be represented by an integral over the time lag of some function f of the variables affecting the processes

$$\int_{t-\tau}^{t} f\{p,\ T,\ \vec{u},\ \vec{u}_l, \ldots\}dt' = E \tag{4.73}$$

The constant E is supposed to be a measure of the level to which the integrated effects must reach in order for vaporization to occur. Almost all applications of the time lag model rest on the assumption that the time lag is sensitive only to the pressure. The function f may then be expanded about its value at the mean pressure,

$$f(p) = f(\bar{p}) + p'\left.\frac{df}{dp}\right|_{\bar{p}} = f(\bar{p})[1 + p'\frac{1}{f(\bar{p})}\left.\frac{df}{dp}\right|_{\bar{p}}]$$

If $f = cp^n$ then $df/dp = ncp^{n-1}$ and $(df/dp)/f(p) = n/p$. The *interaction index* n is defined as

$$n = \frac{\bar{p}}{f(\bar{p})}\left.\frac{df}{dp}\right|_{\bar{p}} \tag{4.74}$$

and $f(p)$ is approximated as

$$f(p) = f(\bar{p})[1 + n\frac{p'}{\bar{p}}] \tag{4.75}$$

This form is now used in approximate evaluation of (4.73).

First differentiate (4.73) with $f(p) = f\{p(t)\}$ to find

$$f\{p(t)\} - (1 - \frac{d\tau}{dt})f\{p(t-\tau)\} = 0$$

Substitution of (4.75) gives

$$1 - \frac{d\tau}{dt} = \frac{1 + n\frac{p'(t)}{\bar{p}}}{1 + n\frac{p'(t-\bar{T})}{\bar{p}}} \approx 1 + n\left[\frac{p'(t)}{\bar{p}} - \frac{p'(t-\tau)}{\bar{p}}\right] \tag{4.76}$$

Set $w_l = \bar{w}_l + w_l'$ in (4.72) and substitute (4.76) to find the basic result of the time lag theory:

$$w_l' = \bar{w}_l n\left[\frac{p'(t)}{\bar{p}} - \frac{p'(t-\tau)}{\bar{p}}\right] \tag{4.77}$$

For analyzing linear stability, $p' = \bar{p}e^{i\bar{\alpha}kt}\psi(\vec{r})$ and $w_l' = \hat{w}_l e^{i\bar{\alpha}kt}$, so

$$\hat{w}_l = \bar{w}_l n(1 - e^{-i\omega\tau})\psi(\vec{r}) \tag{4.78}$$

where the usual approximation has been made, $\alpha\tau << \omega\tau$ in the exponent.

Equation (4.78) is a two-parameter representation of the conversion of liquid to gas. The two parameters, the time lag τ and the interaction or pressure index n, are unknown *a priori*. All work with the time lag theory requires experimental measurements to determine their values. The general idea is simple. After substituting (4.78) in the linearized conservation equations, solution is found for the stability boundary ($\alpha = 0$) with n and τ as parameters. Experimental data for the stability boundary are used to determine n and τ. Crocco, Grey and Harrje in Ref 4.20 were first to obtain sufficient data to confirm the value of this approach. Figure 4.10 reproduces some of their results for the time lag and interaction index inferred from tests with two injectors. The data were taken for the stability boundary of the fundamental longitudinal mode and show the strong dependence on fuel/oxidizer ratio.

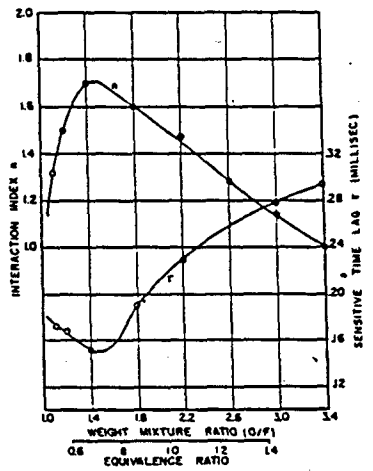

Fig. 11 Values of the sensitive time lag τ and interaction index n determined from the experimental *lower* stability boundary (Fig. 6) for the fundamental longitudinal mode. This figure shows results for the first injector (design O/F = 1.4) at a nominal chamber pressure of 300 psia

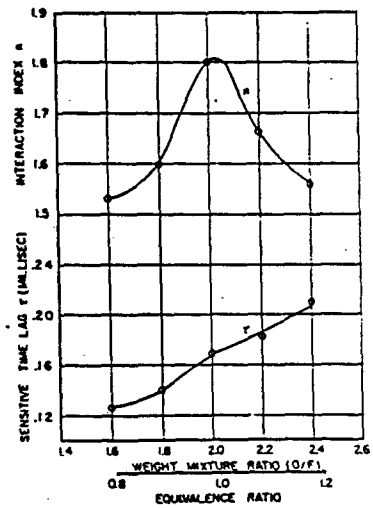

Fig. 12 Experimental values of n and τ for the second injector (design O/F = 2.0)

Figure 4.10

Obviously, there are many limitations. The analysis leading to (4.78) is entirely phenomenological; the final result containing two parameters only is an enormous simplification of the real situation, but there is no way to assess the imperfections.

As an example of the use of the time-lag representation, we summarize some early work using the n-τ model to interpret results computed for the response of vaporization processes to pressure oscillations. Some years after the time-lag model had been developed, work at the NASA Lewis Research Center showed that the stability of a liquid rocket motor could be controlled by varying the characteristics of the vaporization process. The conclusion followed from the results of numerical solutions to the equations for nonlinear unsteady motions in a chamber. The source terms were approximated with models of the atomization, vaporization and burning. Variations of characteristic parameters showed that atomization and vaporization were the dominant rate processes determining the stability limits. That conclusion led to a series of studies particularly emphasizing vaporization.

Because of the difficulty of extracting precise conclusions from numerical analyses, Heidmann and Wieber (Refs. 4.21 and 4.22) devised a method for assessing the vaporization process alone. A droplet is injected

axially in a steady flow. An acoustic field is superimposed having the form of the lowest first tangential mode for a cylindrical chamber ($\sin\theta\ J_1(\kappa_{11}r)$). The motion and vaporization rate of the droplet is calculated throughout its history. By superimposing the results for an array of injected drops, assumed not to interact with one another, one may find the local fluctuation of vaporization rate throughout the chamber. That is the fluctuation of the mass source term w_l in the continuity Eq. (4.33) for the gas phase.

Heidmann and Wieber defined a "response factor," N, to interpret their results:

$$N = \sum \frac{w_l'/\bar{w}_l}{p'/\bar{p}} = \sum \frac{\hat{w}_l/\bar{w}_l}{\hat{p}/\bar{p}} \tag{4.79}$$

where $\sum$ here denotes the sum over all droplets in the volume considered. They gave results for N as a function of various parameters. Typically, N shows a peak of about 0.6–0.9 in a frequency range 0.04–0.1 hertz. Results obtained for n-heptane over fairly wide flow conditions were correlated with a dimensionless parameter containing droplet size, chamber pressure, gas velocity and a dimensionless amplitude of the oscillation.

In a later work, Heidmann and Wieber (Ref. 4.22) used a restricted form of Rayleigh's criterion (described in Section 4.8) and a simpler linear analysis to produce essentially the same conclusions. The new definition of the response factor was

$$N = \sum \frac{\int_0^{2\pi/w} \frac{\hat{w}_l^{(r)}}{\bar{w}_l}\frac{\hat{p}}{\bar{p}}dt}{\int_0^{2\pi/w} \left(\frac{\hat{p}}{\bar{p}}\right)^2 dt} \tag{4.80}$$

These analyses amount to detailed examination of a particular process contributing to the time lag discussed above. Substitution of the real part of (4.78) in (4.80) gives

$$N = n(1 - \cos\omega\tau) \tag{4.81}$$

Heidmann and Wieber found that their numerical results could be approximated quite well in the range $\tau_v\omega < 1$ by the values

$$\begin{aligned} n &= 0.21 \\ \tau &= 4.5\tau_v \end{aligned} \tag{4.82}$$

where τ_v is the mean droplet lifetime. This comparison is shown in Figure 4.11 taken from Heidmann and Wieber (Ref. 4.22).

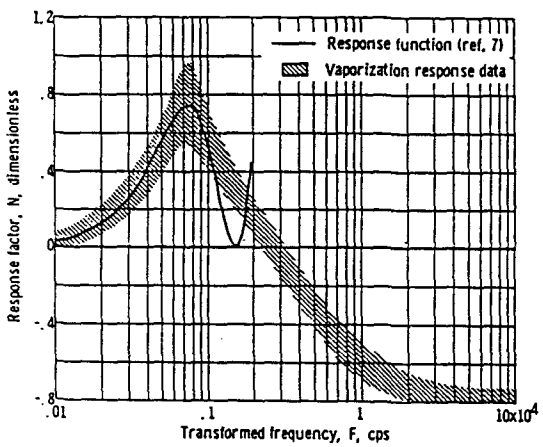

Figure 4.11

Note that the function (4.81) oscillates and therefore becomes a poor approximation for $\omega\tau_v > 1$, as show by the solid line in Figure 4.11. The vaporization rates seem physically reasonable for the conditions shown, so one must conclude that the time lag model fails at higher frequencies. Recently Tong and Sirignano (Ref. 4.23) have re-examined the problem of unsteady vaporization. With their more detailed model including the effects of unsteady heat transfer in the gas phase, they conclude that their vaporization rates are much higher than those found by Heidmann and Weiber.

More strongly, Tong and Sirignano propose that unsteady droplet vaporization is a potential mechanism for driving combustion instabilities. Heidmann and Wieber had earlier noted that the response factor they calculated for the vaporization process was less than that calculated for the nozzle losses. Thus, although vaporization itself did add energy to the acoustic field according to their analysis, the effect was too small to be a mechanism for instabilities. Tong and Sirignano conclude that their results show sufficient energy transfer from the vaporizing droplets to the acoustic field to qualify as a mechanism in actual systems. Their conclusion is based solely on the $p - v$ work done by the process of vaporization and does not include any energy release due to combustion. The proposal is evidently wrong for the following reasons.

It is significant that none of the preceding conclusions involved combustion: the assertion is that coupling between pure vaporization and the acoustic field produces net flow of energy to the oscillations in the gas. The contrary conclusion was reached by Marble and Wooten (Ref 4.24), that both condensing and vaporizing droplets attenuate acoustical motions. The reason for the opposite conclusion seems to be that not all interactions between the droplets and the acoustic field are accounted for in the calculations by Heidmann and Wieber and by Tong and Sirignano.

4.6 APPLICATION OF GREEN'S FUNCTIONS TO LINEAR COMBUSTION INSTABILITIES

With the introduction of a Green's function, a differential equation is converted to an integral equation that is conveniently solved by iteration. The general theory, with applications, is described in many places, notably by Morse and Feshbach (Ref. 4.25, Chapter 10). Culick (Ref. 4.15) first applied the method to problems of combustion instabilities in 1960; it was later adopted by Oberg and Kukula (Ref. 4.26) to study acoustic liners.

Although methods based on Green's functions can be constructed to treat time-dependent problems, practically all applications have been for linear stability. Time-dependent problems are more efficiently handled with the method covered in the next section.

Beginning in the early 1970s, Mitchell and co-workers (see, e.g., Ref. 4.27) introduced the use of a Green's function to produce an integral equation solved by iteration. The time-lag model was assumed to represent the combustion response. Apart from that matter, the method is attractive for analyzing complications such as baffles and resonators that are quite awkward to handle when differential equations are used.

We summarize briefly the method in the form used by Mitchell *et al.* but in the context of the formulation described above in Section 4.3. The problem is to solve the inhomogeneous Eq. (4.60) for the pressure with the boundary condition (4.62). For steady waves, all dependent variables are proportional to $e^{i\bar{k}t}$: $p' = \hat{p}ei\bar{k}t$ and Eq. (4.60) is

$$\nabla^2\hat{p} + k^2\hat{p} = \hat{h} \tag{4.83}$$

where we shall drop all terms h_e and f_e. Define the Green's function satisfying the same equation as $\hat{p}$ but with a unit source at position $\vec{r}_0$ and homogeneous boundary conditions

$$\begin{aligned} \nabla^2 G(\vec{r} \mid \vec{r}_0) + k^2 G(\vec{r} \mid \vec{r}_0) &= \delta(\vec{r} - \vec{r}_0) \\ \hat{n} \cdot \nabla G(\vec{r} \mid \vec{r}_0) &= 0 \end{aligned} \tag{4.84}a,b$$

Now multiply (4.83) by $G(\vec{r} \mid \vec{r}_0)$, (4.84) by $\hat{p}$, integrate over the chamber, use Green's theorem and insert the

boundary conditions (4.62) and (4.84)b to find* the 'solution' for $\hat{p}$:

$$\hat{p} = \int G(\vec{r} \mid \vec{r}_0)\hat{h}(\vec{r}_0)dV_0 + \oiint G(\vec{r} \mid \vec{r}_0)\hat{f}(\vec{r}_0)dS_0 \tag{4.85}$$

It is convenient to express $G(\vec{r} \mid \vec{r}_0)$ as an expansion in the normal modes ψ_n of the system, satisfying Eqs. (4.89)a, b given below. That is, assume the form

$$G(\vec{r} \mid \vec{r}_0) = \sum A_n(\vec{r}_0)\psi_n(\vec{r}_0)$$

Substitution in (4.84)a, multiplication by ψ_n, and integration over the chamber gives

$$A_n = \frac{\psi_n(\vec{r}_0)}{k^2 - k_n^2}$$

so the Green's function is

$$G(\vec{r} \mid \vec{r}_0) = \sum \frac{\psi_m(\vec{r}_0)}{k^2 - k_m^2}\psi_m(\vec{r}) \tag{4.86}$$

Now insert (4.86) in (4.85) and assume that we are examining that mode which, when the perturbations vanish, reduces to the nth classical acoustic mode. Split that term from the remainder of the expansion and apply the normalization $\hat{p} \to \psi_n$ in the limit $\hat{h} = \hat{f} = 0$. Those operations give the formulas for $\hat{p}$ and k^2:

$$\hat{p}(\vec{r}) = \psi_n(\vec{r}) + \sum_{m \neq n} \frac{\psi_m(\vec{r})}{k^2 - k_n^2} \left\{ \int \psi_n(\vec{r}_0)\hat{h}(\vec{r}_0)dV_0 + \oiint \psi_n(\vec{r}_0)\hat{f}(\vec{r}_0)dS_0 \right\} \tag{4.87}$$

$$k^2 = k_n^2 + \frac{1}{E_n^2}\{ \int \psi_n(\vec{r}_0)\hat{h}(\vec{r}_0)dV_0 + \oiint \psi_n(\vec{r}_0)\hat{f}(\vec{r}_0)dS_0 \} \tag{4.88}$$

Equation (4.87) shows explicitly the perturbations of the classical mode shape, ψ_n, giving the actual mode shape $\hat{p}$. Because $\hat{h}$ and $\hat{f}$ depend on p' and $\vec{u}'$ (i.e. $\hat{p}$ and $\hat{\vec{u}}$), Eq. (4.87) is an integral equation for $\hat{p}$ and of course k^2 cannot be calculated with (4.88) until $\hat{p}$ and $\hat{(\vec{r})}$ are known. In the approximate method discussed in the following section, we simply set $\hat{p} \approx \psi_n$, $\hat{\vec{u}} \approx i(\bar{a}/\bar{\gamma}k_n)\nabla\psi_n$ and use (4.88) directly. To proceed further, the integral Eq. (4.87) must be solved. That is where most of the labor in Mitchell's work is expended. He solved the equation numerically using an iteration procedure. We shall not discuss the details further.

We must note, however, that when an iteration procedure is used, care must be exercised that *all* terms of consistent order are retained. The small parameter here is a Mach number, $\overline{M}_r$, characterizing the average flow. Corrections to $\hat{p} = \psi_n$ are thus of order $\overline{M}_r$; that is, if the successive steps in the iteration are labeled $\hat{p}^{(i)}$, the procedure gives:

$$\hat{p}^{(0)} = \psi_n$$
$$\hat{p}^{(1)} = \psi_n + \overline{M}_r\phi^{(1)}$$
$$\hat{p}^{(2)} = \psi_n + \overline{M}_r\phi^{(1)} + \overline{M}_r^2\phi^{(2)} \ldots \text{etc.}$$

The functions h and f are constructed by expansion of the primitive conservation equations according to remarks in Section 4.3. If they are not carried to order higher than $\overline{M}_r$, then it is *not* correct to proceed beyond the zeroth approximation $\hat{p}^{(0)} = \psi_n$ of the mode shape to compute k^2 with (4.88). To carry $\hat{p}$ and $\hat{\vec{u}}$ to higher order than allowed by the construction of $\hat{h}$ and $\hat{f}$ may yield misleading and incorrect results.

---

* In these manipulations, the exchange of variables is made, $\vec{r} \leftrightarrow \vec{r}_0$, and the reciprocity property of G is used: $G(\vec{r} \mid \vec{r}_0) = G(\vec{r}_0 \mid \vec{r})$.

Properly used, the formulation based in Green's function is a powerful method to obtain results for complicated problems. For practical purposes it is much superior to solution of the differential equations owing to the ease with which arbitrary boundary conditions and volumetric sources can be accommodated. In that respect, this method has the same advantages as the approximate method discussed below, except that use of Green's function as described here and in Mitchell's work is strictly limited to linear problems. In contrast, the method now to be constructed can be used to analyze nonlinear behavior.

4.7 SPATIAL AND TIME AVERAGING OF UNSTEADY MOTIONS

Traditional calculations of linear behavior — meaning, almost always, linear stability — are usually based on the differential Eqs. (4.59)a, b, augmented by the linearized equation of state and possibly linearized forms of other equations given in Section 4.2. We shall use in the remainder of this paper the integrated form based on spatial averaging described, for example, by Culick (Refs. 4.28 and 4.19) and Culick and Yang (Ref. 4.30). The fundamental idea is that the actual problem defined by Eq. (4.60) with its boundary condition (4.62) differs in some sense by small amounts from the classical acoustics problem defined by setting $h = f = 0$. That is, the influences of all processes are small perturbations. This formulation, then, has the form naturally suited to an iteration procedure readily constructed by introducing a Green's function as first accomplished by Culick (Ref. 4.15). However, the identical first-order result (the only order legitimately considered with these equations) is obtained more directly in the following way.

4.7.1 Spatial Averaging

The unperturbed problem defines the normal modes, having mode shapes ψ_n and frequencies $\omega_n = \bar{a}k_n$ where k_n is the wavenumber:

$$\begin{aligned} \nabla^2\psi_n + k_n^2\psi_n &= 0 \\ \hat{n}\cdot\nabla\psi_n &= 0 \end{aligned} \qquad (4.89)a, b$$

Then the idea is to compare the perturbed (actual) and unperturbed (classical) problems quite literally by comparing their difference in a spatially averaged sense. Multiply (4.60) by ψ_n, (4.89)a by p', subtract and integrate over the volume of the chamber to give

$$\int \left[\psi_n\nabla^2 p' - p'\nabla^2\psi_n\right] dV - \frac{1}{\bar{a}^2}\int\left[\psi_n\frac{\partial^2 p'}{\partial t^2} - \omega_n^2 p'\psi_n\right] dV = \int \psi_n(h + h_e)dV$$

Upon application of Green's theorem and substitution of the boundary conditions (4.58) and (4.89)b we find

$$\frac{1}{\bar{a}^2}\int\psi_n\left[\frac{\partial^2 p'}{\partial t^2} + \omega_n^2 p'\right] dV = -\left[\int\psi_n h dV + \oiint\psi_n f dS\right] = -\left[\int\psi_n h_e dV + \oiint\psi_n f_e dS\right] \qquad (4.90)$$

The preceding calculations are formally correct and introduce no errors. Now we make the approximation that the pressure field in the actual chamber can be expanded in a series of normal modes for the classical unperturbed problem,

$$p' = \bar{p}\sum_{n=1}^{\infty}\eta_n(t)\psi_n(\vec{r}) \qquad (4.91)$$

The error incurred arises because the $\psi_n(\vec{r})$, and therefore the right-hand side, do not satisfy the correct boundary condition (4.58) set on p' in the actual problem. When the series is used in the integrals above, the error is attenuated, and for other formal reasons not covered here (see, e.g. Morse and Feshback, Ref. 4.25, Chapter 10), this is not as serious an inaccuracy as one might think. We assume also, not a practical constraint, that the normal modes are orthogonal,

$$\int\psi_m\psi_n dV = E_n^2\delta_{mn} \qquad (4.92)$$

Substitution in (4.89) leads finally to the second-order equations for the amplitudes $\eta_n(t)$:

$$\frac{d^2\eta_n}{dt^2} + \omega_n^2\eta_n = F_n + F_{ne} \tag{4.93}$$

and the force is

$$F_n = -\frac{\bar{a}^2}{\bar{p}E_n^2}\left\{\int h\psi_n dV + \oint\!\!\!\oint \psi_n f dS\right\}$$
$$F_{ne} = -\frac{\bar{a}^2}{\bar{p}E_n^2}\left\{\int h_e\psi_n dV + \oint\!\!\!\oint \psi_n f_e dS\right\} \tag{4.94}a,b$$

With proper interpretation and suitable modeling of the processes represented in the functions h, f, h_e, and f_e, the representation of combustion instabilities by Eqs. (4.93) and (4.94)a,b has wide application to all propulsion systems. Relatively little has been done with this formulation applied specifically to liquid rocket engines, but as we shall see shortly, it is quite easy to obtain general results equivalent to those obtained with methods more familiar in this field.

An important point to emphasize is that the approach taken here provides a useful viewpoint as well as a framework useful for both theoretical and practical computations. According to (4.91) and (4.93), any unsteady motion may be regarded as a collection of oscillators, one associated with each normal mode of oscillation appearing in the synthesis (4.91). The problem then comes down to determining the time evolution of the amplitudes $\eta_n(t)$ of the oscillators (modes). Although we have assumed linear motions here, the same formal representation applies to nonlinear motions so long as the amplitudes do not become so large as to violate the approximations taken to give the governing differential equations.

4.7.2 Time Averaging

Combustion instabilities commonly appear as oscillations having slowly varying amplitudes and phases. That is, the fraction changes of amplitude and phase are small in one cycle of the oscillation. Under these circumstances, the method of averaging, or equivalently, expansion in two time scales, can be applied to reduce the set of N second-order Eqs. (4.93), when N modes are considered, to a set of $2N$ first-order equations. That is an enormously useful simplification, and while limits are placed on the range of validity of the results, this step in the method is extremely useful in practice. The limitations are discussed briefly in Section 4.9.2.

According to the behavior just mentioned, we assume that the amplitude $\eta_n(t)$ can be written as

$$\eta_n(t) = r_n(t)\sin[\omega_n t + \phi_n(t)] = A_n \sin\omega_n t + B_n \cos\omega_n t \tag{4.95}$$

where r_n, ϕ_n, A_n, and B_n are slowly varying functions. The simplest, and a physically appealing, way of applying time averaging is a modest variation of averaging developed by Krylov and Bogoliubov (Ref. 4.31). By analogy with a simple mass/spring system, the energy $\mathcal{E}_n$ can be associated with the oscillator governed by Eq. (4.93):

$$\mathcal{E}_n = \frac{1}{2}\omega_n^2\eta_n^2 + \frac{1}{2}\dot{\eta}_n^2 \tag{4.96}$$

The instantaneous velocity of the oscillator is $\dot{\eta}_n$, so that the rate at which work is done on the oscillator is $\dot{\eta}_n F_n$. Averaged over an interval τ at time t, the values are

$$< \mathcal{E}_n >= \frac{1}{\tau}\int_t^{t+\tau} \mathcal{E}_n(t')dt'$$
$$< \dot{\eta}_n F_n >= \frac{1}{\tau}\int_t^{t+\tau} \dot{\eta}_n \mathcal{E}_n F_n dt' \tag{4.97}a,b$$

Conservation of energy for the averaged motion implies that the rate of change of time-averaged energy should equal the time-averaged rate of power in

$$\frac{d}{dt} < \mathcal{E}_n > = < \dot{\eta}_n F_n > \tag{4.98}$$

Because the single function η_n has been replaced by two functions, r_n and ϕ_n, we are free to place a restriction; following Krylov and Bogoliubov, we require

$$\frac{d\phi_n}{dt} r_n \cos(\omega_n t + \phi_n) + \frac{dr_n}{dt} \sin(\omega_n t + \phi_n) = 0 \tag{4.99}$$

Differentiating Eq. (4.95) and enforcing Eq. (4.99) gives the formula for the velocity in the same form as that for a classical conservative oscillator:

$$\dot{\eta}_n = \omega_n r_n \cos(\omega_n t + \phi_n) \tag{4.100}$$

and the energy is

$$\mathcal{E}_n = \frac{1}{2} \omega_n r_n \tag{4.101}$$

With Eq. (4.100), Eq. (4.99) gives

$$\frac{dr_n}{dt} = \frac{1}{\omega_n \tau} \int_t^{t+\tau} F_n \cos(\omega_n t' + \phi_n) dt' \tag{4.102}$$

The equation for $\phi_n(t)$ is found by substituting Eqs. (4.96), (4.100), and (4.99) in the oscillator Eq. (4.98); multiplication by $\sin(\omega_n t + \phi_n)$ and time averaging gives

$$r_n \frac{d\phi_n}{dt} = \frac{-1}{\omega_n \tau} \int_t^{t+\tau} F_n \sin(\omega_n t' + \phi_n) dt' \tag{4.103}$$

It is often more convenient to use the equations for $A_n(t)$ and $B_n(t)$, found by solving Eqs. (4.96), (4.99), (4.102), and (4.103) for $\dot{A}_n(t)$ and $\dot{B}_n(t)$, to give

$$\begin{aligned} \frac{dA_n}{dt} &= \frac{1}{\omega_n \tau} \int_t^{t+\tau} F_n \cos \omega_n t' dt' \\ \frac{dB_n}{dt} &= \frac{-1}{\omega_n \tau} \int_t^{t+\tau} F_n \sin \omega_n t' dt' \end{aligned} \tag{4.104}a,b$$

The assumption that the amplitudes and phases are slowly varying means

$$\begin{aligned} \dot{r}_n \tau << 1 \qquad & \dot{\phi}_n \tau << 2\pi \\ \dot{A}_n \tau << 1 \qquad & \dot{B}_n \tau << 1 \end{aligned} \tag{4.105}$$

These inequalities imply that the functions $A_n(t)$ and $B_n(t)$ will be taken as constant under the integrals in Eq. (4.104).

The original motivation for developing the method of averaging in the form expressed as Eqs. (4.104) and (4.105) was to provide the basis for treating arbitrarily shaped chambers. Differences between geometries are reflected in the unperturbed mode shapes and frequencies. The mode shapes affect the values of parameters that arise in Eqs. (4.104) and (4.105), but the frequency spectrum, as we shall see, influences the qualitative

of the equations. It appears that the derivation of Eqs. (4.104) and (4.105) is not restricted to particular geometries, but, to date, these results have been applied only to the simplest case of longitudinal modes for which the harmonic frequencies are integral multiples of the fundamental. Application to other cases requires further calculations, which we will not pursue here; preliminary examination suggests some difficulties that have not been resolved.

Culick (Ref. 4.28) has shown that F_n has the following form for second-order acoustics:

$$F_n = -\sum_{i=1}^{\infty}[D_{ni}\dot{\eta}_i + E_{ni}\eta_i] - \sum_{i=1}^{\infty}\sum_{j=1}^{\infty}[A_{nij}\dot{\eta}_i\dot{\eta}_j + B_{nij}\eta_i\eta_j] \tag{4.106}$$

The constants D_{ni}, E_{ni}, A_{nij}, and B_{nij} depend on the unperturbed mode shapes and frequencies; the D_{ni} and E_{ni} arise from linear processes and are usually proportional to the Mach number of the mean flow. (A notable exception arises with the presence of condensed material. The characteristic parameter then depends on the properties of the particles.) Consider the linear terms only. Substitution of Eq. (4.106) in Eq. (4.104), with τ equal to the period of the nth mode, leads to the following results:

$$\left(\frac{dA_n}{dt}\right)_{\text{linear}} = -\frac{1}{2}D_{nn}A_n + \frac{1}{2}\frac{E_{nn}}{\omega_n}B_n \tag{4.107}$$

$$\left(\frac{dB_n}{dt}\right)_{\text{linear}} = -\frac{1}{2}D_{nn}B_n + \frac{1}{2}\frac{E_{nn}}{\omega_n}A_n \tag{4.108}$$

Multiply the first of these by A_n and the second by B_n, and add the results to find the equation for the amplitude, $\dot{r}_n = (D_{nn}/2)r_n$, where $r_n^2 = A_n^2 + B_n^2$. Thus, $r_n \sim \exp(\alpha_n t)$, with $\alpha_n = -D_{nn}/2$, the growth constant for the nth mode.

Now, from the definition (4.95) of $\eta_n(t)$, we find

$$A_n \approx e^{\alpha_n t}\cos\phi_n \qquad B_n \approx e^{\alpha_n t}\sin\phi_n$$

Substitution in Eqs. (4.107) and (4.108) leads to the identification $E_{nn}/2\omega_n = \dot{\phi}_n$. But $\dot{\phi}_n$ can be interpreted as the frequency shift in the nth mode that is due to the perturbations because the perturbed frequency is

$$\omega = \frac{d}{dt}(\omega_n t + \phi_n) = \omega_n + \dot{\phi}_n = \omega_n + (\omega - \omega_n)$$

Hence we have established the two rules that the growth constant for the nth mode is 1/2 the coefficient of $\dot{\eta}_n$ in the form (4.107), and the frequency shift is $1/2\omega_n$ times the coefficient of η_n:

$$\alpha_n = -\frac{1}{2}D_{nn} \tag{4.109}$$

$$\theta_n = -(\omega - \omega_n) = -\frac{1}{2}\frac{E_{nn}}{\omega_n} \tag{4.110}$$

These rules are often conveniently applied after a representation of a particular process has been constructed.

4.8 RESULTS FOR LINEAR STABILITY

We remarked earlier that there is really only one problem of linear stability and within the present analysis it is readily solved. According to the principles of Fourier analysis, with essentially no practical restrictions, any function can be synthesized as a finite or infinite series of orthogonal functions. Here, we apply the idea to a pressure record represented as a sum of the normal modes $\psi_n(\vec{r})$ of a chamber, with time-dependent amplitudes $\eta_n(t)$, Eq. (4.91). That representation presumes neither linear nor nonlinear behavior. If the behavior is linear, as we shall assume, and the modes are uncoupled, as we also assume, then it is a familiar

result that to find the time-dependent properties of the normal modes, the amplitudes may be assumed to vary exponentially in time:

$$\eta_n(t) = \hat{\eta}_n e^{i\omega_n t} \qquad \text{(normal modes)} \tag{4.111}$$

Hence we assume that the normal modes are neither driven nor damped. Finding the normal modes requires solving the classical problem of the scalar wave equation in a closed volume having the same shape as the combustion chamber in question except that the exhaust nozzle is closed at its entrance. Both the mode shapes $\psi_n(\vec{r})$ and the natural frequencies are found in this calculation, the solution to (4.89)a, b.

For the actual problem with all relevant processes accounted for, the form (4.111) is again assumed, and for the problem of linear stability, the amplitudes are assumed to have the form

$$\eta_n(t) = \hat{\eta}_n e^{i\bar{a}K_n t} \qquad \text{(linear stability)} \tag{4.112}$$

where the actual complex wavenumber is

$$K_n = \frac{1}{\bar{a}}(\Omega_n - i\alpha_n) \tag{4.113}$$

Now the perturbed mode corresponding to the n^{th} classical mode may either grow ($\alpha_n > 0$) or decay ($\alpha_n < 0$) in time. The actual frequency is

$$\Omega_n = \omega_n + \delta\omega_n \tag{4.114}$$

Hence the problem of linear stability comes down to determining for each perturbed mode the frequency shift $\delta\omega_n$ and the growth constant α_n. The basis for the calculation is the linearized form of the equations already treated.

Substitute (4.112) - (4.114) in Eq. (4.93), with $F_{ne} = 0$ to find

$$(\Omega_n - i\alpha_n)^i = \omega_n^2 + \frac{\hat{F}_n}{\hat{\eta}_n}$$

where, for linear behavior, we write $h = \hat{h}e^{i\bar{a}K_n}$, $f = \hat{f}e^{i\bar{a}K_n}$, so $F_n = \hat{F}_n e^{i\bar{a}Kn}$. For the usual case, $\alpha_n << \Omega_n$ and $\Omega_n - \omega_n << 1$, which must be satisfied to be consistent with approximations already made. Then separating the real and imaginary parts of the last equation, with the definition (4.96)a gives

$$\begin{aligned}
\Omega_n &= \omega_n - \frac{\bar{a}^2}{2\omega_n \bar{p} E_n^2}\left\{\int \frac{\hat{h}^{(r)} + \hat{h}_e^{(r)}}{\hat{\eta}_n}\psi_n dV + \oint\!\!\oint \frac{\hat{f}^{(r)} + \hat{f}_e^{(r)}}{\hat{\eta}_n}\psi_n dS\right\} \\
\alpha_n &= \frac{\bar{a}^2}{2\omega_n \bar{p} E_n^2}\left\{\int \frac{\hat{h}^{(i)} + \hat{h}_e^{(i)}}{\hat{\eta}_n}\psi_n dV + \oint\!\!\oint \frac{\hat{f}^{(i)} + \hat{f}_e^{(i)}}{\hat{\eta}_n}\psi_n dS\right\}
\end{aligned} \tag{4.115}a, b$$

in which $(\ )^{(r)}$ and $(\ )^{(i)}$ denote real and imaginary parts. These two formulas are the solution to the problem of linear stability. In particular, setting $\alpha_n = 0$ defines the stability boundary in terms of the various parameters arising in the functions h and f. That result is the basis for the Standard Stability Prediction program (Nickerson *et al.*, Ref. 4.32) written for the U.S. Air Force and widely used by industrial and governmental organizations to analyze the stability of motions in solid propellant rockets.

4.8.1 Rayleigh's Criterion

Probably the most widely quoted general principal in the field of combustion instabilities is Rayleigh's criterion formulated by Rayleigh in 1878:

> *"If heat be periodically communicated to, and abstracted from, a mass of air vibrating (for example) in a cylinder bounded by a piston, the effect produced will depend upon the phase of the vibration*

at which the transfer of heat takes place. If heat be given to the air at the moment of greatest condensation, or be taken from it at the moment of greatest rarefaction, the vibration is encouraged. On the other hand, if heat be given at the moment of greatest rarefaction, or abstracted at the moment of greatest condensation, the vibration is discouraged."

Roughly the gist of the principle is that heat addition tends most strongly to drive acoustic waves if the energy is added in the region of space where the oscillating pressure reaches greatest amplitude and is in phase. Suppose that the heat release associated with combustion is simply proportional to the pressure, so the fluctuation $Q' = \beta(p'/\bar{p})$ where β is a complex constant. Suppose further that only one mode is present, so we write $p' = \bar{p}\eta_n(t)\psi_n(\vec{r})$, a single term of the expansion (4.111). The simplest case is a steady oscillation, and $\eta_n(t) = \hat{\eta}_n e^{i\omega_n t}$. Write $\beta = |\beta|e^{i\phi_Q}$ and the oscillation of heat addition is

$$Q' = |\beta|Q_o\hat{\eta}_n\psi_n(\vec{r})e^{i(\omega_n t+\phi_Q)} \tag{4.116}$$

Rayleigh's criterion then states that heat addition is most destabilizing if the fluctuation Q' is in phase with the pressure oscillation, $\phi_Q = 0$. The assumed form already ensures that the magnitude of the oscillation of heat addition is maximum where the pressure oscillation has maximum amplitude. Although the principle seems fairly obviously true, these remarks do not serve as proof. The formulation described above can be used not only to establish the criterion but also to extend its application to all processes and nonlinear behavior (see Culick, Refs. 4.29 and 4.33). Zinn (Ref. 4.34) has also recently discussed Rayleigh's criterion, but only for linear heat addition.

We take advantage of the fact that each acoustic mode has an associated oscillator having unit mass and natural frequency ω_n, whose motion (i.e. time evolution of its amplitude η_n) is described by Eq. (4.93). The energy of a simple oscillator is the sum of its kinetic and potential energies,

$$\mathcal{E}_n = \frac{1}{2}\left(\dot{\eta}_n^2 + \omega_n^2\eta_n^2\right) \tag{4.117}$$

We interpret Rayleigh's criterion to be a statement concerning the change $\Delta\mathcal{E}_n$ of the energy in one cycle. The product of the force $(F_n + F_{ne})$ times the velocity $\dot{\eta}_n$ is the power input, so

$$\Delta\mathcal{E}_n(t) = \int_t^{t+\tau_n} (F_n + F_{ne})\dot{\eta}_n dt' \tag{4.118}$$

In general $\Delta\mathcal{E}_n(t)$ varies with time, increasing from cycle to cycle for an unstable mode.

Indeed, for linear motions, if all processes are taken into account, $\Delta\mathcal{E}_n$ is proportional to the growth constant α_n and this extended form of Rayleigh's criterion is equivalent to the principle of linear stability (Refs. 4.29 and 4.33),

$$\Delta\mathcal{E}_n = 2\pi\omega_n\alpha_n \tag{4.119}$$

Thus the precise form of Rayleigh's criterion stated above is found by taking only the part of F_n representing heat addition and setting $F_{ne} = 0$. The result is (Ref. 4.33)

$$\Delta\mathcal{E}_n(t) = (\alpha - 1)\frac{\omega_n^2}{\bar{p}E_n^2}\int \psi_n dV \int_t^{t+\tau_n} \eta_n Q' dt' \tag{4.120}$$

in which Q' must be expressed in terms of real quantities. Thus, instead of the complex form we write in the case Q' proportional to p',

$$Q' = Q_o\psi_n(\beta_1\eta_n + \beta_2\dot{\eta}_n) \tag{4.121}$$

where β_1, β_2 are real. The formula (4.120) leads to

$$\Delta\mathcal{E}_n = \pi(\alpha - 1)\beta_1\omega_n Q_o \tag{4.122}$$

Combination of (4.119) and (4.120) gives the convenient formula for the growth constant due to heat addition,

$$\alpha_n = \frac{(\alpha-1)\omega_n}{2\pi\bar{p}E_n^2}\int \psi_n dV \int_0^{\tau_n} \eta_n Q' dt' \tag{4.123}$$

where we have used the fact that $\eta_n Q'$ has period $\tau_n = 2\pi/\omega_n$ to shift the limits of the integral. We should also note that whereas the time derivative $\partial Q'/\partial t$ appears as the source in the wave Eq. (4.60) and in the oscillator Eqs. (4.93), Q' itself occurs in (4.120) and (4.123), also a consequence of periodicity as explained in Ref 4.33.

4.9 ANALYSIS OF NONLINEAR BEHAVIOR

Considerable effort has been spent, for more than four decades, on experimental and analytical programs devoted to solving problems of combustion instabilities. Much of the work has been required to measure quantities which, because of the complex processes involved, cannot be predicted accurately from first principles. Analytical work has been concerned largely with linear behavior, the chief purpose being to predict stability of small disturbances in combustion chambers. Many useful results have been obtained, serving in practice to help design experiments, correlate data, and estimate the stability of new systems.

In theory, the problem of linear stability is essentially solved and well-understood; in practice the situation is quite different. The reason is that the information required to predict stability is always imperfectly known. Predictions therefore carry with them substantial inaccuracies. Moreover, it is difficult to obtain reliable data for the growth or decay rates of small disturbances in operating engines. Few results are available.

The situation in respect to nonlinear behavior of liquid rocket engines is quite different. The theory is far more difficult, contains a broad array of important problems, and is only in the beginning stages of development. Yet it is the nature of combustion instabilities that almost all data show significant nonlinear behavior. Indeed, the most important means of assessing the stability of liquid rocket engines — observation of the physical behavior following initiation of finite explosive charges ('bombing') — involves intrinsically nonlinear behavior. The theory of bombing, really the theory of nonlinear instabilities (sometimes called 'triggering') hardly exists and has produced no useful results.

For application to combustion instabilities, there are two fundamental problems to be integrated:

(1) the conditions under which an *unstable* linear system will execute a stable limit cycle;

(2) the conditions under which a *stable* linear system can be caused, by suitable disturbance, to execute a stable limit cycle.

Both of these problems were discussed for simple cases in Section 4.1 where we emphasized that a linearly unstable motion in a combustion chamber must normally be viewed as a self-excited system: an unstable motion therefore reaches finite amplitude only through the action of nonlinear processes. That is the substance of problem (1). Problem (2) is the problem of 'bombing' or 'triggering.' In the language of dynamical systems theory, problem (1) arises from a supercritical bifurcation and problem (2) from a sub-critical bifurcation.

We summarize briefly some of the recent results based on the analytical framework described in Section 4.7. Only nonlinear gasdynamics is accounted for, although it is well known that other nonlinear processes are significant — possibly essential — to explain some of the observed behavior. The reason for focusing on nonlinear gasdynamics is that, in a practical sense, this is the only nonlinear process that is known with full confidence. This the approach taken in recent work has been to understand as completely as possible the consequences and influences of the nonlinear gasdynamics. Differences from observed behavior should then, presumably, be ascribed to other processes. In liquid rocket engines, it seems probable that the next most important processes are those accomplishing the conversion of injected liquid to gases *prior* to combustion. Although ultimately the energy supplied to both the mean and unsteady flows must be generated by combustion, it appears likely that the chemical kinetics and burning processes are not normally the dominant tie-dependent processes in propulsion systems.

Despite its potential importance, nonlinear modeling of time-dependent injection processes (Section 4.4.2) remains in an unsatisfactory primitive state with virtually no detailed models available for use in the sort of approximate analysis described here. The time-lag model covers the matter, but for reasons explained in Section 4.5, that is not an informative basis for understanding combustion instabilities in either a fundamental or practical sense.

Before discussing the more recent results, we review briefly previous analyses other than numerical simulations. The following discussion is taken from the review by Culick (Ref. 4.35). Long before the work producing the approximate analysis reviewed here, much attention had been directed to nonlinear combustion instabilities. That the phenomena are intrinsically nonlinear was recognized practically from the earliest experimental results. In 1956, motivated partly by the common occurrence of transverse waves in combustors, Maslen and Moore (Ref. 4.36) treated finite amplitude waves, based on a power series expansion in the amplitude, but with no combustion and mean flow. Flandro (Ref. 4.37) extended that work to include combustion and flow, and succeeded in explaining the origin of roll torques observed occasionally in solid rockets.

Chu (Ref. 4.38) and Chu and Ying (Ref. 4.39) treated the problem of thermally driven nonlinear longitudinal oscillations with shock waves in a closed tube using the method of characteristics. Although the heat source was allowed to be sensitive to pressure in part of that work, no combustion and flow were accounted for.

Motivated partly by laboratory tests of gas-fueled rockets at Princeton, the first detailed analysis of the problem with combustion and flow was published by Sirignano (Ref. 4.40) and Sirignano and Crocco (Ref. 4.41), also using the method of characteristics, modified to include coordinate stretching following the PLK (Poincaré–Lighthill–Kuo) procedure. That work was followed by further analyses of longitudinal waves by Mitchell *et al.*(Ref. 4.42) and by Crocco and Mitchell (Ref. 4.43) using different methods allowing treatment of distributed combustion. At the same time, Zinn (Ref. 4.44) examined nonlinear behavior of transverse modes, based on expansion of the equation for the velocity potential in powers of the amplitude.

Those early works by the Princeton group were first to address quantitatively the broad subject of nonlinear motions in a combustion chamber. They were also first to expose some particular problems which remain unsolved in general, notably the possible existence of stable limit cycles and the conditions under which 'triggering' to stable or unstable limit cycles may occur. Apparently for at least three reasons, the approaches taken during the 1960s have not been pursued further by researchers outside the Princeton school: (1) particularly with the method of characteristics, the calculations become so detailed and divorced from physical behavior as to obscure understanding; (2) except in the analysis by Crocco and Mitchell (Ref. 4.43), the combustion zone was assumed to be thin and located at the end of the chamber, physically a serious limitation if one seeks general applications; and (3) perhaps more seriously, the 'time-lag model' of the combustion processes is used. It is true that any linear unsteady combustion process can be represented by a time-lag model, in practice amounting to definition of a transfer function. However, a serious difficulty arises with the usual assumption implied in all the works cited above, that the time lag is independent of frequency. That is rarely true. For example, it is known that the time lag is a critically strong function of frequency for unsteady burning of a solid propellant, being dominated by transient heat transfer in the condensed phase.

Nonlinear behavior of a dynamical system is both qualitatively and quantitatively dependent on the values of the parameters characterizing the linear behavior. Generalizations from particular results are almost never possible without actually performing the necessary analysis. Therefore, there is presently almost no basis for claiming generality for any of the results involving the time-lag model of linear behavior, however useful the model may be for other purposes.

The introduction by Zinn and Powell (Ref. 4.45) of the use of Galerkin's method to study instabilities in liquid rockets, and later applied by Zinn and Lores (Ref. 4.46) and Lores and Zinn (Ref. 4.47) marked an important shift of emphasis on the type of analytical methods used in this field. As in the earlier works, the time-lag model of combustion is used, so the results are similarly restricted. However, the general approach, pursued independently by Culick (Ref. 4.28) for application to solid rockets, will accommodate very general representations of all nonlinear processes.

The discussion in Section 4.1, appealing to simple models, serves as an introduction to the more elaborate behavior found with solutions to the equations derived in Sections 4.3 and 4.7. We emphasize again that only gasdynamic nonlinearities are considered here. Although related work is still in progress, much understanding has been gained. Probably the most important conclusion is that while stable limit cycles can be found to exist in a broad range of conditions with *only* nonlinear gasdynamics, it appears that if no other nonlinear processes are present, the motions in a combustion chamber are not nonlinearly unstable. That is, at least one mode must be linearly unstable in order for limit cycles to exist.

4.9.1 Limit Cycles

Most of the results for limit cycles have been obtained for longitudinal modes and second-order acoustics (i.e. quadratic nonlinearities in the fluctuations). For any geometry, F_n defined by (4.94)a has the form (4.106):

$$F_n = -\sum_{i=0}^{\infty}[D_{ni}\dot{\eta}_i + E_{ni}\eta_i] - \sum_{i=1}^{\infty}\sum_{j=1}^{\infty}[A_{nij}\dot{\eta}_i\dot{\eta}_j + B_{nij}\eta_i\eta_j] \tag{4.124}$$

Purely longitudinal modes have the important special characteristic that the unperturbed natural frequencies are integral multiples of the fundamental. As a result, the double series in F_n reduces to a single series, and the first-order equations obtained with time averaging become

$$\frac{dA_n}{dt} = \alpha_n A_n + \theta_n B_n + \frac{n\beta}{2}\sum_{i=1}^{\infty}\Big[A_i\left(A_{n-i} - A_{i-n} - A_{i+n}\right) - B_i\left(B_{n-i} + B_{i-n} - B_{i+n}\right)\Big]$$

$$\frac{dB_n}{dt} = -\theta_n A_n + \alpha_n B_n + \frac{n\beta}{2}\sum_{i=1}^{\infty}\Big[A_i\left(B_{n-i} + B_{i-n} - B_{i+n}\right) + B_i\left(A_{n-i} - A_{i-n} + A_{i+n}\right)\Big] \tag{4.125}a,b$$

where $\alpha_n = -D_{nn}/2$, $\theta_n = -E_{nn}/2\omega_n$ and

$$\beta = \frac{\bar{\gamma}+1}{8\bar{\gamma}}\omega_1 \tag{4.126}$$

Although actual systems rarely show $\omega_n = n\omega_1$ exactly, there are many instances, particularly of solid and liquid rockets, when the spectrum of frequencies closely satisfies this condition. Hence this special case has received much attention since it was first studied by Culick (Ref. 4.28). Prior to that time, no formal theory existed to explain the observed occurrences of steady nonlinear periodic oscillations, i.e. limit cycles; calculations of limit cycles had been carried out in earlier works cited above, but analytical results had not been obtained owing to the nature of the methods used.

Most attention was therefore directed to discovering first whether limit cycles could be predicted, and second the conditions determining their existence and stability. Note that the constant β can be absorbed as a scaling parameter (β^{-1} is a time scale) so that all of the behavior — linear and nonlinear — is determined by the values of the linear parameters (α_n, θ_n), which contain completely the influences of all linear processes. In the earliest work, the existence of limit cycles was established by solving Eqs. (4.125)a,b numerically for ranges of the linear parameters.

Confidence in the approximate analysis was gained quite early with successful comparisons and numerical solutions to the partial differential equations (Levine and Culick, Refs. 4.48 and 4.49). Several problems were examined, including development of a disturbance into a weak shock wave (no combustion or mean flow), decay of large amplitude waves due to the presence of condensed material, and the growth of a combustion instability to a limit cycle in a solid rocket. Using more efficient numerical routines developed by Levine and Baum (Ref. 4.50), Culick and Yang (Ref. 4.30) have reported the example shown in Figure 4.12 showing the waveform in a limit cycle computed with the numerical and approximate analysis (for five modes). The frequencies (shifted due to perturbations) and the amplitudes of the modes are predicted quite well by the approximate analysis as Table 4.1 shows.

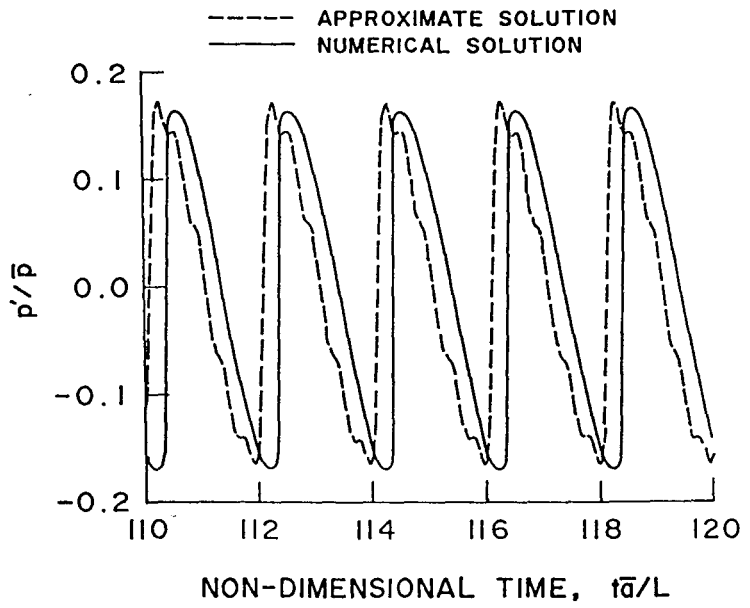

Figure 4.12

			Frequency		
Mode	1	2	3	4	5
Numerical	926	1824	2698	3595	4491
Approximate	895	1785	2683	3571	4449
			Amplitude $\lvert p'/\bar{p}\rvert$		
Mode	1	2	3	4	5
Numerical	0.151	0.042	0.234	0.0203	———
Approximate	0.151	0.0478	0.0280	0.0153	0.0188

Table 4.1

The frequencies agree within 3%, illustrating the familiar fact that accurate prediction of frequencies is not a demanding test of an approximate analysis — good approximations should (as here) be built into the formulation. More to the point is the good agreement of the amplitudes except for the highest ($n = 5$) mode. The reason for the higher approximate values is that truncation to five modes eliminates energy transfer to higher modes where it is ultimately dissipated. We shall see that the intrinsic tendency for energy transfer upwards is an important fundamental property of these problems, having a strong influence on the development of limit cycles from small initial disturbances.

While it is useful to be able to obtain results of this sort — inexpensive and accurate approximations to nonlinear behavior — this is only part of the story. It is perhaps even more significant both theoretically and practically, to establish the qualitative dependence of nonlinear behavior on the linear parameters. The special

structure of the nonlinear Eqs. (4.124)a, b allows considerable progress in that respect. Awad and Culick (Ref. 4.51) reported the first formal results for existence and stability of limit cycles for purely longitudinal modes, using Eqs. (4.124)a, b, although as noted above, the question had previously been primarily addressed with numerical solutions. Closed form results have been obtained only for the case of two modes; here we only describe the gist of the matter.

For two modes, Eqs. (4.124)a, b become

$$\begin{aligned}
\frac{dA_1}{dt} &= \alpha_1 A_1 + \theta_1 B_1 - \beta(A_1 A_2 - B_1 B_2) \\
\frac{dB_1}{dt} &= \alpha_1 B_1 - \theta_1 A_1 + \beta(B_1 A_2 - A_1 B_2) \\
\frac{dA_2}{dt} &= \alpha_2 A_2 + \theta_2 B_2 + \beta(A_1^2 - \beta_1^2) \\
\frac{dB_2}{dt} &= \alpha_2 B_2 - \theta_2 A_2 + 2\beta B_1 A_1
\end{aligned} \qquad (4.127)a, b, c, d$$

Limit cycles correspond to equilibrium states for this system. There are two possible cases: $\dot{A}_n = \dot{B}_n = 0$, or $A_n = a_n \cos(\nu_n t + \psi_n)$, $B_n = a_n \sin(\nu_n t + \psi_n)$. In the first case, the functions A_n, B_n are constant in the limit cycle and in the second case they oscillate, with frequencies ν_n. The two possibilities were first discovered in the numerical calculations reported by Culick (Ref. 4.28) and confirmed theoretically by Awad and Culick (Ref. 4.51).

The analysis then proceeds as follows. First substitute in (4.127)a, b, c, d the assumed forms for the A_n, B_n in the limit cycle and solve the algebraic equations. It is a consequence of the special structure of those equations that formulas for the amplitudes can be derived, simultaneously with conditions for their existence. Let subscript $(\,)_0$ denote values in the limit cycle; then for the case when the amplitudes are constant in the limit cycle, the results may be written:

$$\begin{aligned}
A_{10} &= \frac{1}{\beta}\left[-\alpha_1\alpha_2\left(1 + \frac{\theta_1^2}{\alpha_1^2}\right)\right]^{\frac{1}{2}} \\
B_{10} &= 0 \\
A_{20} &= \frac{1}{\beta}\alpha_1 \\
B_{20} &= \frac{1}{\beta}\theta_2
\end{aligned} \qquad (4.128)a, b, c, d$$

These formulas are not unique. Because there is an arbitrary phase on the limit cycle, one constant is undetermined; here its value has been fixed by setting $B_{10} = 0$.

If the amplitudes are allowed to oscillate in the limit cycle, producing a small shift in the modal frequencies, then

$$A_n = a_n \cos(\nu_n t + \psi_n); \quad B_n = a_n \sin(\nu_n t + \psi_n) \qquad (4.129)$$

The frequency shifts are found to be

$$\nu_1 + \frac{1}{2}\nu_2 = -\frac{\alpha_1\theta_2 + \alpha_2\theta_1}{2\alpha_2 - \alpha_2}$$

and the maximum amplitudes are

$$\begin{aligned}
a_1 &= \left\{-\frac{\alpha_1\alpha_2}{\beta_2}\left[1 + \left(\frac{2\theta_1 - \theta_2}{2\alpha_1 + \alpha_2}\right)^2\right]\right\}^{\frac{1}{2}} \\
a_2 &= \frac{\alpha_1}{\beta}\left[1 + \left(\frac{2\theta_1 - \theta_2}{2\alpha_1 + \alpha_2}\right)^2\right]^{\frac{1}{2}}
\end{aligned} \qquad (4.130)a, b$$

Because A_{10}, Eq. (4.128)a, and a_1, Eq. (4.130)a, must be real, one necessary condition for existence is

$$\alpha_1 \alpha_2 < 0 \tag{4.131}$$

The physical interpretation of this condition follows from the meaning of the α_n as growth or decay constants. If α_n is positive (negative) then in the linear approximation, energy is added (lost) to the n^{th} mode. Hence (4.131) represents the requirement the one mode must gain energy and one must lose energy in order that the oscillations should reach a steady sustained amplitude. If both α_1 and α_2 are negative, the system is absolutely stable, and if α_1 and α_2 are both positive, the motions grow without limit. The nonlinear terms in (4.125)a, b, and hence in (4.127)a, b, c, cause transfer of energy from one mode to another.

Conditions for stability of the limit cycles are determined by examining the evolution of small disturbances from the stationary states. A set of inequalities is deduced from application of the Routh-Hurwitz or Lienard criteria to the characteristic polynomial. Figure 4.13 (taken from Ref. 4.52) shows one way of displaying the results in terms of the linear parameters. Ranges of the parameters for which stable limit cycles exist are indicated by the hatched lines.

It seems remarkable that simple conditions of existence and stability can be obtained for transverse modes, in a cylindrical chamber, by following the same approach used to treat longitudinal modes. The reason is that the time-averaged equations again have a special structure allowing the calculations to be carried out again for two modes. What makes this surprising is that because the natural frequencies do not satisfy the condition $\omega_n = n\omega_1$, the time-averaged equations contain modulation on the right-hand side.

Before averaging, use of (4.124) leads to the set of equations valid for second-order acoustics,

$$\begin{aligned}
\frac{dA_n}{dt} = &- \frac{1}{2\omega_n} \sum_{i=1}^{\infty} \Big\{ C_{ni} \left[\cos(\omega_n + \omega_i)t + \cos(\omega_n - \omega_i)t\right] \\
&\qquad + S_{ni} \left[\sin(\omega_n + \omega_i)t - \sin(\omega_n - \omega_i)t\right] \\
&- \frac{1}{2\omega_n} \sum_{i=1}^{\infty} \sum_{j=1}^{\infty} \Big\{ F_{nij} a_{ij} \left[\cos(\omega_n + \omega_{ij+})t + \cos(\omega_n - \omega_{ij+})t\right] \\
&\qquad + G_{nij} b_{ij} \left[\cos(\omega_n + \omega_{ij+})t + \cos(\omega_n - \omega_{ij+})t\right] \\
&\qquad - F_{nij} d_{ij} \left[\sin(\omega_n + \omega_{ij+})t - \sin(\omega_n - \omega_{ij+})t\right] \\
&\qquad + G_{nij} e_{ij} \left[\sin(\omega_n + \omega_{ij-})t - \sin(\omega_n - \omega_{ij-})t\right] \Big\}
\end{aligned} \tag{4.132}$$

where

$$\begin{aligned}
\omega_{ij+} &= \omega_i + \omega_j & \omega_{ij-} &= \omega_i - \omega_j \\
C_{ni} &= \omega_i D_{ni} A_i + E_{ni} B_i & S_{ni} &= -\omega_i D_{ni} B_i + E_{ni} A_i \\
F_{nij} &= \omega_i \omega_j A_{nij} - B_{nij} & G_{nij} &= \omega_i \omega_j A_{nij} + B_{nij} \\
a_{ij} &= \frac{1}{2}(A_i A_j - B_i B_j) & b_{ij} &= \frac{1}{2}(A_i A_j + B_i B_j) \\
d_{ij} &= \frac{1}{2}(A_i B_j + AjBi) & e_{ij} &= \frac{1}{2}(A_i B_j - A_j B_i)
\end{aligned}$$

A similar equation defines $\dot{B}_n$; see Yang and Culick (Ref. 4.53) where further details of the analyses and the numerical values of the coefficients F_{nij} and G_{nij} are given. Three modes are considered: the first and second tangential and the first radial having the following wave numbers and mode shapes:

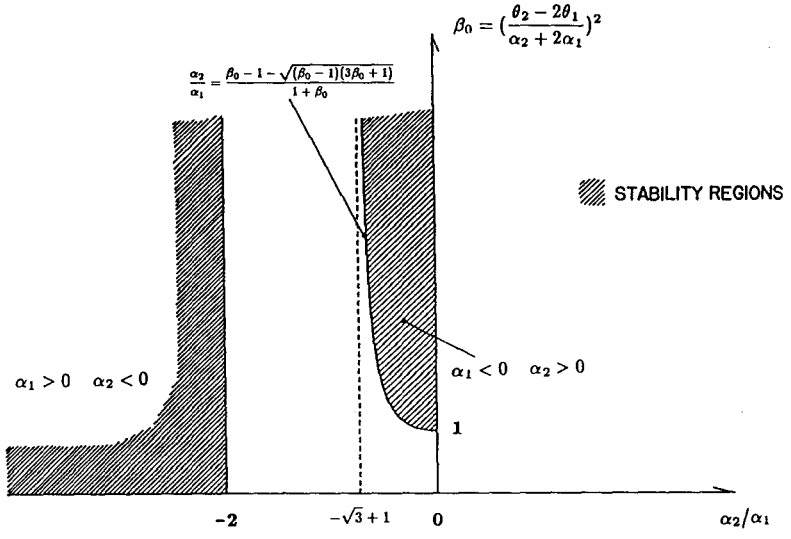

Figure 4.13

First Tangential Mode (1T)

$$\kappa_1 R = 1.8412 \qquad \psi_1 = \cos\theta J_1(\kappa_1 r) \qquad \psi_4 = \sin\theta J_1(\kappa_1 r) \tag{4.133}$$

First Radial Mode (1R)

$$\kappa_2 R = 3.8317 \qquad \psi_2 = J_0(\kappa_2 r) \tag{4.134}$$

Second Tangential Mode (2T)

$$\kappa_3 R = 3.0542 \qquad \psi_3 = \cos 2\theta J_2(\kappa_3 r) \qquad \psi_5 = \sin 2\theta J_2(\kappa_3 r) \tag{4.135}$$

Degeneracy of the tangential modes leads to the existence of standing or spinning waves, but here we consider only standing waves.

One interesting feature is that the coefficients F_{nnn} and G_{nnn} associated with nonlinear gasdynamical self-coupling are nonzero only for the first radial mode. However, these are eliminated in the averaging process so, as in the case of purely longitudinal modes, there is apparently no significant self-coupling. Absence of self-coupling is a qualitative property of the problem that has significant consequences in respect to nonlinear stability.

The averaged equations for A_n and B_n are:

First Tangential Mode (1T)

$$\frac{dA_1}{dt} = \alpha_1 A_1 + \theta_1 B_1 + 2\left[a_1 b_{12}\cos\Omega_1 t + a_2 b_{13}\cos\Omega_2 t\right] + 2\left[a_1 a_{12}\sin\Omega_1 t + a_2 a_{13}\sin\Omega_2 t\right] \tag{4.136}$$

$$\frac{dB_1}{dt} = -\theta_1 A_1 + \alpha_1 B_1 - 2\left[a_1 b_{12}\sin\Omega_1 t + a_2 b_{13}\sin\Omega_2 t\right] + 2\left[a_1 a_{12}\cos\Omega_1 t + a_2 a_{13}\cos\Omega_2 t\right] \tag{4.137}$$

First Radial Mode (1R)

$$\frac{dA_2}{dt} = \alpha_2 A_2 + \theta_2 \beta_2 + b_1 \left[(A_1^2 - B_1^2) \cos \Omega_1 t - 2 A_1 B_1 \sin \Omega_1 t \right] \tag{4.138}$$

$$\frac{dB_2}{dt} = -\theta_2 A_2 + \alpha_2 B_2 + b_1 \left[(A_1^2 - B_1^2) \sin \Omega_1 t + 2 A_1 B_1 \cos \Omega_1 t \right] \tag{4.139}$$

Second Tangential Mode (2T)

$$\frac{dA_3}{dt} = \alpha_3 A_3 + \theta_3 B_3 + b_2 \left[(A_1^2 - B_1^2) \cos \Omega_2 t - 2 A_1 B_1 \sin \Omega_2 t \right] \tag{4.140}$$

$$\frac{dB_3}{dt} = \alpha_3 B_3 - \theta_3 A_3 + b_2 \left[A_1^2 - B_1^2) \sin \Omega_2 t + 2 A_1 B_1 \cos \Omega_2 t \right] \tag{4.141}$$

where

$$a_1 = 0.1570 \left(\frac{\bar{a}}{R} \right) \qquad a_2 = -0.0521 \left(\frac{\bar{a}}{R} \right)$$

$$b_1 = -0.1504 \left(\frac{\bar{a}}{R} \right) \qquad b_2 = 0.1873 \left(\frac{\bar{a}}{R} \right)$$

and

$$\Omega_1 = 2\omega_1 - \omega_2 = -0.1493 \left(\frac{\bar{a}}{R} \right) \qquad \Omega_2 = 2\omega_1 - \omega_3 = 0.6282 \left(\frac{\bar{a}}{R} \right) \tag{4.142}$$

Note particularly that all of the nonlinear terms on the right-hand sides of equations (4.136) - (4.141) contain modulation factors oscillating at either Ω_1 or Ω_2.

Solutions for two combinations of two modes have been obtained: first tangential and first radial modes (1T/1R); and first and second tangential modes (1T/2T). For the case (1T/1R), write A_n and B_n in terms of an amplitude and phase:

$$A_n = r_n(t) \cos \Phi_n(t) \qquad B_n = r_n(t) \sin \Phi_n(t) \tag{4.143}$$

and substitute in (4.136) - (4.141). Dropping terms dependent on the second tangential mode leads to the system

$$\frac{dr_1}{dt} = \alpha_1 r_1 + a_1 r_1 r_2 \cos \left(2\Phi_1 - \Phi_2 + \Omega_1 t \right) \tag{4.144}$$

$$\frac{dr_2}{dt} = \alpha_2 r_2 + b_1 r_1^2 \cos \left(2\Phi_1 - \Phi_2 + \Omega_1 t \right) \tag{4.145}$$

$$\frac{d\Phi_1}{dt} = -\theta_1 - a_1 r_2 \sin \left(2\Phi_1 - \Phi_2 + \Omega_1 t \right) \tag{4.146}$$

$$\frac{d\Phi_2}{dt} = -\theta_2 + b_1 \frac{r_1^2}{r_2} \sin \left(2\Phi_1 - \Phi_2 + \Omega_1 t \right) \tag{4.147}$$

The fact that all right-hand sides contain the same time-varying argument, $2\Phi_1 - \Phi_2 + \Omega_1 t$ is crucial to producing simple results.

In the limit cycle, the amplitudes r_{no} are constant, and their values are found as the solutions to the algebraic equations given by setting to zero the left-hand sides of (4.144) - (4.147). The results are

$$r_{10} = \sqrt{\frac{\alpha_1 \alpha_2}{a_1 b_1}} \left[1 + \left(\frac{2\theta_1 - \theta_2 - \Omega_1}{2\alpha_1 + \alpha_2} \right)^2 \right]^{\frac{1}{2}} \tag{4.148}$$

$$r_{20} = -\frac{\alpha_1}{a_1} \left[1 + \left(\frac{2\theta_1 - \theta_2 - \Omega_1}{2\alpha_1 + \alpha_2} \right)^2 \right]^{\frac{1}{2}} \tag{4.149}$$

Because $a_1 b_1$ is negative (see the values given above), $\alpha_1 \alpha_2$ must be negative to make r_{10} real. The physical reason is the same as that explained in connection with the same result (4.131) for longitudinal modes.

Just as for longitudinal modes, we must allow for frequency shifts in the limit cycle. Eventually the results are found for the time-dependent amplitudes η_{no}:

$$\eta_{10} = r_{10} \sin[(\omega_1 + \nu_1)t + \zeta_1]$$
$$\eta_{20} = r_{20} \sin[2(\omega_1 + \nu_1)t + \zeta_2] \qquad (4.150)a,b$$

where

$$2\zeta_1 - \zeta_2 = \tan^{-1}\left[\frac{(\omega_2 - \theta_2) - 2(\omega_1 - \theta_1)}{2\alpha_1 + \alpha_2}\right] \qquad (4.151)$$

We can set either ζ_1 or ζ_2 equal to zero because zero phase is arbitrary. In the limit cycle, the participating motions must have frequencies that are integral multiples of the fundamental in order that the motion be periodic. That (4.150)a,b satisfy this requirement is a partial confirmation that the approximations used in the averaging process are correct. The result was found also by Zinn and Powell (Ref. 4.45) in their numerical analysis of transverse modes. Figure 4.14 (taken from Ref. 4.53) shows two examples of limit cycles for this case; the values of the limiting amplitudes are independent of the initial conditions.

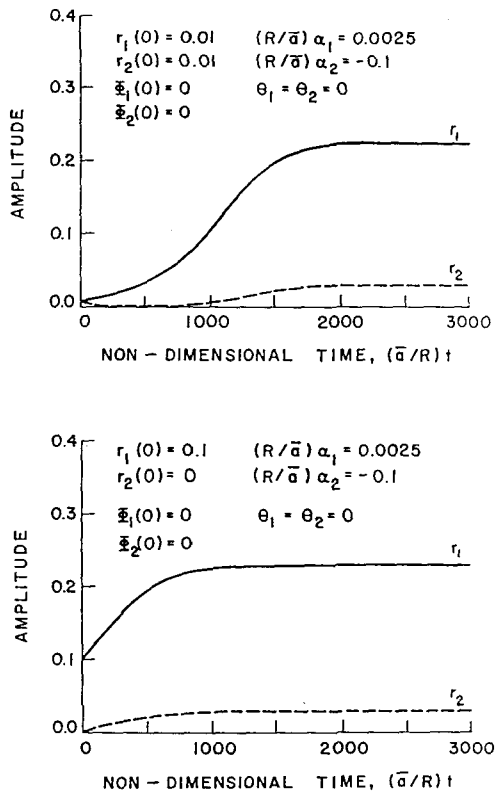

Figure 4.14

Establishing the conditions for stability of the limit cycles follows the procedure outlined in the preceding section. The necessary and sufficient conditions are

$$\alpha_1\alpha_2 < 0$$
$$\alpha_1 + \alpha_2 < 0 \qquad (4.152)a,b,c$$
$$2\alpha_1 + \alpha_2 < 0$$

For $\alpha_1 < 0$ the additional condition must be met

$$\alpha_1 > \frac{-|K|}{2+\xi}\left[\frac{-\xi^2+2\xi+2}{\xi^2+2\xi+2}\right]^{\frac{1}{2}} \qquad (4.153)$$

where $K = 2\theta_1 - \theta_2 - \Omega_1$ and $\xi = \alpha_2/\alpha_1$ must lie in the range $1-\sqrt{3} < \xi < 0$.

Similar results have also been found for the case (1T/2T). Moreover, the case of three modes (1T, 2T, 1R) can be solved for the amplitudes in the limit cycle but simple formulas defining the stability of those limit cycles cannot be found.

4.9.2 Application of Bifurcation Theory and a Continuation Method

The approximate analysis described here is intended to serve two main purposes: to provide an efficient means of performing routine calculations for analysis and design; and to furnish a theoretical framework within which observed behavior of combustion instabilities may be understood. Even with the formal representation reduced to a set of coupled first-order equations, it is difficult to extract the sort of qualitative information necessary to satisfactory understanding. Accordingly, much effort has been expended in the past few years on the simplest possible case, the approximate model in which only two modes are accounted for. It is remarkable, a consequence of the special form of the gasdynamical nonlinearities, that simple explicit results can be obtained for a useful variety of special problems, as we have seen in the preceding section.

Because of its simplicity, the two-mode approximation based on time-averaging is an attractive basis for studying the nonlinear characteristics of combustion instabilities. This model can of course also accommodate other nonlinear processes, although presently results are available only for nonlinear gasdynamics. Within the model itself, it is impossible to assess the limits of validity, or the general consequences of, the two basic features defining the model: truncation of the modal expansion (4.91) to two terms; and time-averaging. One way of checking the accuracy of the results is to compare directly with results of numerical simulations, as in the example given for longitudinal modes in Section 4.9.1.

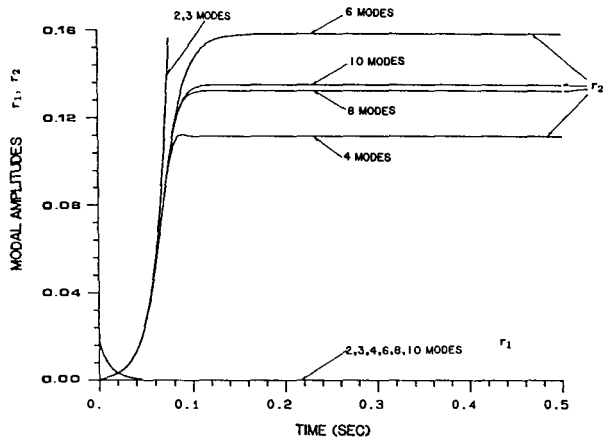

Figure 4.15

Some effects of truncation can be discovered simply by solving a succession of problems, increasing the number of modes with the same linear parameters α_n, θ_n. What one finds depends in the first instance where the values for α_1, θ_1, α_2, θ_2 lie on the stability diagram for limit cycles. Figure 4.15 (taken from Ref. 4.52) shows that, for example, a limit cycle unstable in the two-mode approximation can, under some circumstances, be made stable by accounting for more modes. One conceivable strategy would be a survey of special cases, solving the time-averaged equations and the second-order oscillator equations, with and without modal truncation.

It becomes an immense task to discover all possible sorts of behavior due to the large number of parameters: for a given geometry, there are two for each mode considered plus whatever quantities are introduced* by nonlinear processes. That is why exact solutions, such as those for the two-mode approximation, are so important. However, only a few exact solutions have been found, and only for problems restricted in three important aspects already noted: the only nonlinear process is gasdynamics; the modal expansion is truncated to a small number of modes; and the time-averaged equations have been used. For both theoretical purposes and for practical applications it is essential to avoid these restrictions.

In the absence of analytical solutions, it is necessary to resort to numerical methods. Numerical simulations for the system of coupled oscillators can be carried out without serious difficulties, but that is an expensive procedure. It is more efficient and productive of useful information to apply a continuation method for computing stationary states (e.g. limit cycles) of the dynamical system as one or more parameters are changed. Well known in other fields, the approach has been adapted by Jahnke and Culick (Ref. 4.54) to investigate nonlinear combustion instabilities. The procedure is broadly the following, for the case of longitudinal modes and only nonlinear second-order acoustics.

First the system (4.93) of oscillator equations is put in the form

$$\dot{x} = f(x, \mu(\epsilon)) \tag{4.154}$$

where x is a vector of dependent variables (the state vector), μ represents the parameters (α_n, θ_n), and ϵ is a small parameter, here of the order of the average Mach numbers. After rescaling time, $t \rightarrow \omega_1 t$ and defining the variable $\delta_n = \dot{\eta}_n$, the equations (4.93) with F_n written for longitudinal modes, can be put in the form (4.154), with $x = (\eta_n,\ \delta_n)$:

$$\begin{aligned}
\dot{\eta}_n &= \delta_n \\
\dot{\delta}_n &= -n^2\eta_n + 2\alpha_n\delta_n + 2n\theta_n\eta_n \\
&= -\sum_{i=1}^{n-1}\left[C_{ni}^{(1)}\delta_i\delta_{n-i} + D_{ni}^{(1)}\eta_i\eta_{n-i}\right] \\
&= -2\sum_{i=1}^{\infty}\left[C_{ni}^{(2)}\delta_i\delta_{n-i} + D_{ni}^{(2)}\eta_i\eta_{n+i}\right]
\end{aligned} \tag{4.155}$$

To obtain numerical results, the modal expansion must be truncated at some number of modes $n = N$. Following the method outlined in Section 4.7, or similar procedures, the system (4.155) can also be time averaged. By carrying out calculations for both (4.155) and the time-averaged system, and for increasing $N \geq 2$, it is then possible to determine the consequences of modal truncation and time averaging.

The next step is to determine the stationary states defined by $\dot{x} = 0$, the solution to

$$f(x, u) = 0 \tag{4.156}$$

or the corresponding time-averaged equation. This is of course exactly what was done in Section 4.9.1 to determine the existence of limit cycles. In general, solving (4.156), which is a set of N coupled nonlinear

* Note that nonlinear gas dynamics alone does not bring any new parameters, in addition to those set by the geometry, if the mean flow is not accounted for.

equations, becomes difficult. A continuation method (we have used that worked out by Doedel and Kernevez, Ref. 4.55) is a recipe for finding the values of the dependent variables x_0 defining the stationary states as the parameters μ are varied ('continued') from some initial values. At each stage, after the values of μ have been changed, the stability of the new stationary state is determined by computing the eigenvalues of the Jacobian matrix arising in the linearized problem. That process also identifies bifurcations.

Use of a continuation method does not resolve the difficulty of determining the behavior over broad ranges of many parameters. However, the procedure does impose a certain systematic approach and yields much more information than one obtains from numerical simulations alone. One example makes the point.

The two-mode approximation with time averaging produces the result summarized in Figure 4.13 for longitudinal modes: stable limit cycles exist only if the values of the parameters α_n, θ_n $(n = 1, 2)$ lie in certain ranges defined by a stability boundary. It is not possible within that restricted analysis to state whether the presence of the stability boundary is intrinsic to the physical mode, or is due to the approximations of modal truncation and/or time averaging. With the continuation method we have partly resolved the question. For a particular set of fixed parameters $(\theta_1, \alpha_2, \theta_2)$ and α_1 varied, the stability region for the original equations without time averaging is reduced and in fact a turning point bifurcation appears as α_1 is increased from zero.

More interestingly and significant is the result, again for fixed values of the other parameters, the stability boundary apparently does not exist if enough modes are accounted for. Figure 4.15 already suggests the possible importance of truncation. With the continuation method, the effect of truncation can be found in straightforward fashion. The values of all parameters except α_1 are fixed ($\alpha_n < 0$ for $n \geq 2$) and α_1 is varied from zero so the first mode is linearly unstable. Figures 4.16 and 4.17 show the amplitudes for the cases of two modes and four modes. With the averaged equations and the two-mode approximation, the amplitudes become infinite when $\alpha_1 = 131$ (i.e. on the stability boundary). However, the second-order equations have a turning-point bifurcation at $\alpha_1 = 131$, Figure 4.16.

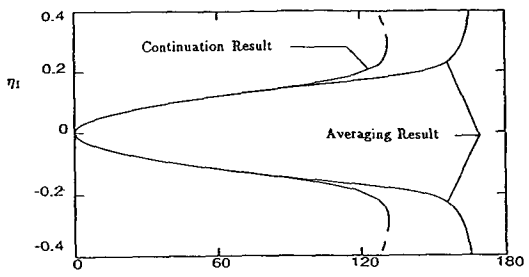

(a) Maximum amplitude of η_1

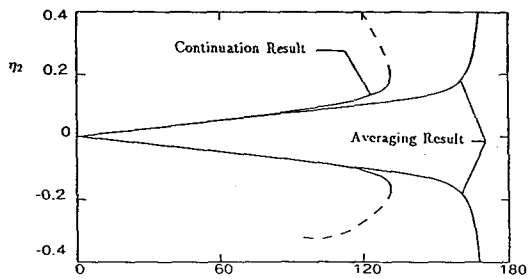

(b) Maximum amplitude of η_2

Figure 4.16

In contrast, when four modes are accounted for, as shown in Figure 4.17, there is neither a stability boundary nor a bifurcation for α_1 less than 300. No results have been computed in this case for the time-averaged equations although other examples suggest that the region of stability is at least expanded when more modes are included.

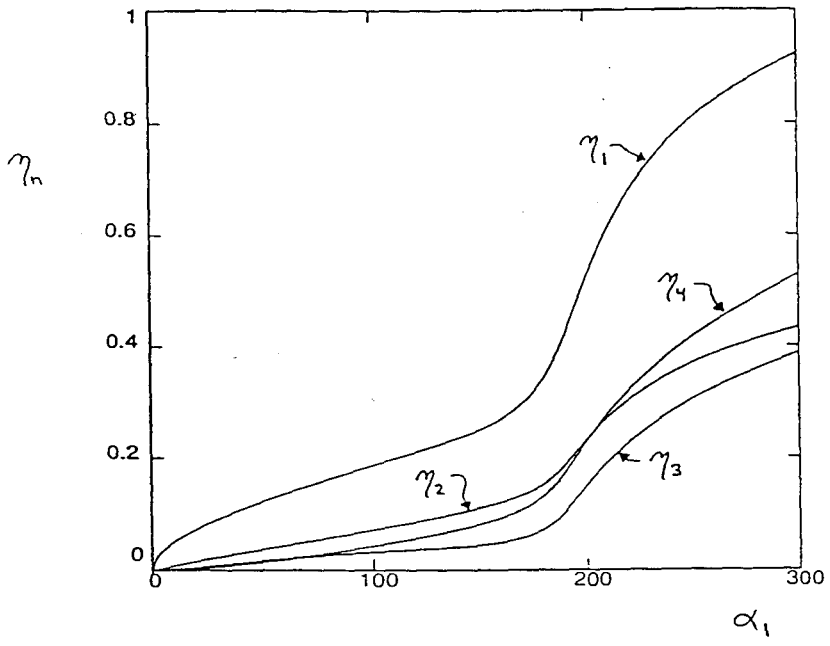

Figure 4.17

Further details and examples are given by Jahnke and Culick (Ref. 4.54). It seems at this time that the application of a continuation method offers the best means of understanding the global behavior of the dynamical system (4.93) representing combustion instabilities. Work is in progress to include other nonlinear processes and to obtain results for modes other than purely longitudinal.

4.9.3 Nonlinear Instabilities ('Triggering')

Aside from their technical significance in the field of unsteady combustion, nonlinear instabilities have two practical applications: first, any real engine becomes unstable when exposed to a sufficiently strong internal disturbance, a phenomenon important to understand; and second, stability rating, the method used in the U.S. to rate the resistance of linearly stable engines to triggering, is understandable only in the context of nonlinear instabilities.

In the grand scheme of this subject, theory, analysis, and laboratory work should establish the laws governing unsteady behavior, scaling laws, dependence on geometry, and other parameters defining linear and nonlinear behavior. If the task could be carried to completion, then the basis would exist for minimum development costs of stable engines, with test programs planned mainly to confirm expected performance and stability. The actual case is far from the ideal and important testing procedures devised to establish stability characteristics of engines remain an important — and expensive — part of any development program. Those procedures define the process called 'stability rating.'

As in much of this subject, NASA report SP-194 (Ref. 4.56) remains the most complete reference for stability. Little seems to have changed in the past 20 years except for the improvements in instrumentation,

data acquisition, and data processing. Although there are other methods used to investigate special aspects of stability (e.g. oscillations involving the propellant supply system), we shall discuss briefly here only the two basic methods used routinely to determine the stability of high-frequency wave modes in a chamber. 'Bombing' a chamber by initiating small explosive charges is the older of the two, having been introduced in the 1950s; the second method is called 'temperature ramping' in which the temperature of one of the propellants, usually the fuel, is increased more or less linearly in time until an unstable motion develops spontaneously, or, less commonly, the transient following a small explosion becomes a sustained oscillation. Because there is ample guidance available for applying these methods, nothing is added here by elaborating details. Rather, we shall only try to provide a general context with examples.

We have emphasized that there are two general kinds of stability: linear and nonlinear. 'Stability rating' in the linear sense means determining the stability boundary in some space of parameters. For example, when the n-τ model of unsteady combustion in used, the essential parameters are of course n and τ. However, as explained in Section 4.4.5, the values of n and τ can only be inferred as functions of parameters that can be controlled experimentally, such as oxidizer-fuel ratio or geometrical properties of the chamber. Determining n and τ from experimental work requires a model (normally that producing Eq. (4.78) and a linear stability theory giving two formulas for n and τ. Thus the procedure is truly semi-empirical, based on a mixture of theoretical and observational results. As used in engine development, methods of stability do not appeal to any theoretical results. A limited number of parameters are changed (the size of explosive charge or the propellant temperature) and the stability of motions is then assumed in some simple terms such as rate of decay or growth of oscillations or perhaps just growth or decay. Frequency shifts are normally small, or cannot be interpreted meaningfully, so the best one can do in rating linear stability is to determine the rate of growth or decay.

For rocket engines, the only practical means of assessing nonlinear stability is based on detonating small explosive charges. A typical strategy involves a sequence of charges, increasing in size to reach a condition when the disturbance no longer decays but continues as more-or-less periodic large-amplitude motions. Empirical rules have been constructed to define what constitutes acceptable dynamic stability of a chamber.

Nonlinear stability or instability is intrinsically a far more difficult matter than linear stability. There is no satisfactory, comprehensive theory for nonlinear combustion instabilities although much is known in respect to the stability of nonlinear dynamical systems generally. 'Nonlinear instability' means that a linearly stable system becomes unstable to a sufficiently large disturbance. In the field of combustion instabilities, we are concerned with systems that contain sources and sinks of energy. The problem of nonlinear instability is therefore not simply an elaboration of the motion of a rotating pendulum in a gravitational field; in that case, small initial disturbances produce small-amplitude to-and-fro oscillations, but sufficiently large disturbances cause the pendulum to execute continuing circular motions.

For practical applications, the general problem of nonlinear instability is the most important unsolved theoretical problem in this field. There is no reason to question the validity of the approximate analysis as a framework for investigating this phenomenon. Furthermore, with the great advances in dynamical systems theory accomplished in the recent past, all necessary methods of solution are available. Thus we conclude that the primary realistic obstacle to obtaining results is modeling the dominant nonlinear processes which, we contend, as we emphasized earlier in this section, are likely those classified here as injection processes.

ACKNOWLEDGEMENTS

This review is based on work accomplished with many students and colleagues in the past twenty-five years. Support has been provided chiefly by NASA, the U.S. Navy, the U.S. Air Force, consulting arrangements with various firms in the rocket industry, and by the California Institute of Technology.

REFERENCES

4.1) Rubin, S., "Longitudinal Instability of Liquid Rockets Due to Propulsion Feedback (POGO)," *AIAA J. Spacecraft,* Vol. 3, No. 8, August 1966, pp. 1188–1195.

4.2) Dordain, J.J., Lourme, D., and Estoueig, C., "Etude de l'Effet POGO sur les Lanceurs EUROPA II et DIAMANT B," *Acta Astronautica*, Vol. 1, 1974, pp. 1357–1384.

4.3) Souchier, A., Lemoine, J.C. and Dorville, G., "Résolution du Problème des Instabilities sur le Moteur Viking," IAF Paper No. 82-363, 33^{rd} IAF Congress, 1982, Paris.

4.4) *First International Symposium on Liquid Rocket Engine Instability (Proceedings)*, The Pennsylvania State University, January 18–20, 1993.

4.5) Oefelein, J.C. and Yang, V., "A Comprehensive Review of Liquid-Propellant Instabilities in F-1 Engines," Dept. of Mech. Eng., Propulsion Engineering Research Center, The Pennsylvania State University, July 1992.

4.6) Wu, P.-K., Hsiang, L.P., and Faeth, G.M., "Aerodynamic Effects on Primary and Secondary Spray Breakup," *First International Symposium on Liquid Rocket Engine Instability (Proceedings)*, The Pennsylvania State University, January 18–20, 1993.

4.7) Vingert, L., Gicquel, P., Lourme, D., and Ménoret, L., "Coaxial Injectors, Atomization," *First International Symposium on Liquid Rocket Engine Instability (Proceedings)*, The Pennsylvania State University, January 18–20, 1993.

4.8) Hsieh, K.C. Shuen, J.S., and Yang, V., "Droplet Vaporization in High-Pressure Environments, I: Near Critical Conditions," *Combustion Science and Technology*, Vol. 76, 1991, pp. 111–132.

4.9) Shuen, J.S., Yang, V., and Hsiao, C.C., "Combustion of Liquid-Fuel Droplets in Supercritical Conditions," *Combustion and Flame*, Vol. 89, 1992, pp. 299–319.

4.10) Yang, V., Hsieh, K.C., and Shuen, J.S., "Supercritical Droplet Combustion and Related Transport Phenomena," *AIAA 31^{st} Aerospace Sciences Meeting*, Paper No. AIAA 93-0812, 1993.

4.11) Tsien, H.S., "The Transfer Functions of Rocket Nozzles," *J. Am. Rocket Soc.*, Vol. 22, 1952, pp. 139–143.

4.12) Crocco, L. "Supercritical Gas Discharge With High Frequency Oscillations," *Aerotechnica*, Vol. 33, 1953, pp. 46–53.

4.13) Crocco, L. and Cheng, S.I. *Theory of Combustion Instability in Liquid Propellant Rocket Motors*, AGARDoraph No. 8, Butterworths Scientific Publications, London.

4.14) Crocco, L., Monti, R., and Grey, J., "Verification of Nozzle Admittance Theory by Exact Measurement of the Admittance Parameter," *ARS J.*, Vol. 31, No. 6, pp. 771–775.

4.15) Culick, F.E.C., "High Frequency Oscillations in Liquid Rockets," *AIAA J.*, Vol. 1, No. 5, 1963, pp. 1097–1104.

4.16) Crocco, L. and Sirignano, W.A., "Behavior of Supercritical Nozzles Under Three-Dimensional Oscillatory Conditions," AGARDograph No. 117, 1967.

4.17) Summerfield, M., "A Theory of Unstable Combustion in Liquid Propellant Rocket Systems," *ARS J.*, Vol. 21, No. 5, 1951, pp. 108–114.

4.18) Gunder, D.F. and Friant, D.R., "Stability of Flow in a Rocket Motor," *J. App. Mech.*, Vol. 17, No. 3, 1950, pp. 327–333.

4.19) Dipprey, D.F., "Liquid Propellant Rockets," in *Chemistry in Space Research* (R.F. Landel and A. Rembaum, Eds.), American Elsevier Publishing, Inc., 1972.

4.20) Crocco, L., Grey, J., and Harrje, D.T., "Theory of Liquid Propellant Rocket Combustion Instability and Its Experimental Verification," *ARS J.*, Vol. 30, No. 2, 1960, pp. 159–168.

4.21) Heidmann, M.F. and Wieber, P.R., "Analysis of n-Heptane Vaporization in Unstable Combustor With Traveling Transverse Oscillations," NASA TN D-3424, 1966.

4.22) Heidmann, M.F. and Wieber, P.R., "Analysis of Frequency Response Characteristics of Propellant Vaporization," NASA TN D-3749, 1966.

4.23) Tong, A.Y. and Sirignano, W.A., "Vaporization Response of Fuel Droplet in Oscillatory Field," ASME National Heat Transfer Conference, Paper No. 87-HT-58, 1987.

4.24) Marble, F.E. and Wooten, D.C., "Sound Attentuation in a Condensing Vapor," *Physics of Fluids*, Vol. 13, 1970, pp. 2657–2664.

4.25) Morse, P.M. and Feshbach, H., *Methods of Theoretical Physics*,

4.26) Oberg, C.L. and Kukula, N.M., "Analysis of the F-1 Acoustic Liner," *J. Spacecraft*, Vol. 8, No. 12, 1971, pp. 1138–1143.

4.27) Mitchell, C.E. and Eckert, K. (1979) "A Simplified Computer Program for the Prediction of the Linear Stability Behavior of Liquid Propellant Combustors," NASA CR-3169, 1979.

4.28) Culick, F.E.C., "Nonlinear Behavior of Acoustic Waves in Combustion Chambers," Parts I and II, *Acta Astronautica*, Vol. 3, 1976, pp. 714–757.

4.29) Culick, F.E.C., "Combustion Instabilities in Liquid-Fueled Propulsion Systems — An Overview," ADARD 72B PEP Meeting, 1988.

4.30) Culick, F.E.C. and Yang, V., "Prediction of the Stability of Unsteady Motions in Solid Propellant Rocket Motors," Chapter 18 in *Nonsteady Burning and Combustion Stability of Solid Propellants*, Progress in Astronautics and Aeronautics (L. de Luca, E. W. Price, and M. Summerfield, Eds.), 1992.

4.31) Krylov, N. and Bogoliubov, N., *Introduction to Nonlinear Mechanics*, Princeton University Press, 1947.

4.32) Nickerson, G. R., Culick, F.E.C., and Dang, L.G., "Standard Stability Prediction Method for Solid Rocket Motors, Axial Mode Computer Program, User's Manual," Software and Engineering Associates, Inc., report prepared for Air Force Rocket Propulsion Laboratory, AFRPL–TR–83–017, 1983.

4.33) Culick, F.E.C., "A Note on Rayleigh's Criterion," *Combustion Science and Technology*, Vol. 56, 1987, pp. 159–166.

4.34) Zinn, B. T., "Pulsating Combustion," Chapter 2 in *Advanced Combustion Methods,* F.J. Weinber (Ed.), Academic Publishers, London, 1986.

4.35) Culick, F.E.C., "Some Recent Results for Nonlinear Acoustics in Combustion Chambers," AIAA 13^{th} Aeroacoustics Conference, AIAA Paper No. 90-3927. To be publisjed in *AIAA J.*

4.36) Maslen, S.H. and Moore, F K., "On Strong Transverse Waves Without Shocks in a Circular Cylinder," *J. Aero. Science,* Vol. 23, pp. 583–593, 1956.

4.37) Flandro, G.A., *Rotating Flows in Acoustically Unstable Rocket Motors*, Ph.D. Thesis, Daniel and Florence Guggenheim Jet Propulsion Center, California Institute of Technology, 1967.

4.38) Chu, B.T., "Analysis of a Self-Sustained Thermally Driven Nonlinear Vibration ," *The Physics of Fluids,* Vol. 6, No. 11, pp. 1638–1644, 1963.

4.39) Chu, B.-T. and Ying, S.J., "Thermally Driven Nonlinear Oscillations in a Pipe with Traveling Shock Waves," *The Physics of Fluids,* Vol. 6, No. 11, pp. 1625–1637, 1963.

4.40) Sirignano, W.A., *A Theoretical Study of Nonlinear Combustion Instability: Longitudinal Mode*, Ph.D. Thesis, Department of Aerospace and Mechanical Sciences, Princeton University, 1964.

4.41) Sirignano, W.A. and Crocco, L., "A Shock Wave Model of Unstable Rocket Combustors," *AIAA Journal*, Vol. 2, No. 7, pp. 1285–1296, 1964.

4.42) Mitchell, C.E., Crocco, L., and Sirignano, W.A., "Nonlinear Longitudinal Instability in Rocket Motors with Concentrated Combustion," *Combustion Science and Technology*, Vol. 1, pp. 269–274, 1969.

4.43) Crocco, L. and Mitchell, C.E., "Nonlinear Periodic Oscillations in Rocket Motors with Distributed Combustion," *Combustion Science and Technology*, Vol. 1, pp. 147–169, 1969.

4.44) Zinn, B.T., "A Theoretical Study of Nonlinear Combustion Instability in Liquid-Propellant Rocket Engines," *AIAA Journal*, Vol. 6, No. 10, pp. 1966–1972, 1968.

4.45) Zinn, B.T. and Powell, F.A., "Nonlinear Instability in Liquid-Propellant Rocket Engines," *Thirteenth Symposium (International) on Combustion*, pp. 491–503, 1971.

4.46) Zinn, B.T. and Lores, E.M., "Application of the Galerkin Method in the Solution of Nonlinear Axial Combustion Instability Problems in Liquid Rockets," *Combustion Science and Technology*, Vol. 4, pp. 269–278, 1972.

4.47) Lores, E.M. and Zinn, B.T., "Nonlinear Longitudinal Instability in Rocket Motors," *Combustion Science and Technology*, Vol. 7, pp. 245–256, 1973.

4.48) Levine, J.L. and Culick, F.E.C., "Numerical Analysis of Nonlinear Longitudinal Combustion Instability in Metalized Solid-Propellant Rocket Motors," Vol. 1, Analysis and Results, Ultrasystems, Inc., report prepared for the Air Force Rocket Propulsion Laboratory, AFRPL–72–88, 1972.

4.49) Levine, J.L. and Culick, F.E.C., "Nonlinear Analysis of Solid Rocket Combustion Instability," Ultrasystems, Inc., report prepared for the Air Force Rocket Propulsion Laboratory, AFRPL–74–74–45, 1974.

4.50) Levine, J.L. and Baum, J.D., "A Numerical Study of Nonlinear Instability Phenomena in Solid Rocket Motors," *AIAA Journal*, Vol. 21, No. 4 (April), pp. 557–564, 1983.

4.51) Awad, E. and Culick, F E.C., "On the Existence and Stability of Limit Cycles for Longitudinal Acoustic Modes in a Combustion Chamber," *Combustion Science and Technology*, Vol. 46, pp. 195–222, 1986.

4.52) Lord Rayleigh, "The Explanation of Certain Acoustical Phenomena," *Royal Institution Proceedings*, Vol. VIII, pp. 536–542, 1878. See also *The Theory of Sound*, Dover Publications, Vol. II, p. 226, 1945.

4.53) Yang, V. and Culick, F.E.C., "On the Existence and Stability of Limit Cycles for Traverse Acoustic Oscillations in a Cylindrical Combustion Chamber, I. Standing Modes," *Combustion Science and Technology*, Vol. 72, pp. 37–65, 1990.

4.54) Jahnke, C.C. and Culick, F.E.C., "An Application of Dynamical Systems Theory to Nonlinear Combustion Instabilities," AIAA 31st Aerospace Sciences Meeting, AIAA Paper 93–0114, 1993.

4.55) Doedel, E.J. and Kernevez, J.P., *Software for Continuation Problems in Ordinary Differential Equations with Applications*, Applied Mathematics Publication 217–50, California Institute of Technology, 1984.

4.56) Harrje, D.J. and Reardon, F.H. (Eds.), *Liquid Propellant Rocket Instability*, NASA SP–194, 1972.